"Исследование структуры адронной и ядерной материи в процессах с x_T~1 и в кумулятивной области"

С.С.Шиманский

Программу исследований с пучками антипротонов можно рассматривать как продолжение исследований проводимых и планируемых в ЛФВЭ.

Как мы можем зарегистрировать состояние адронной (ядерной) материи с плотностью значительно большей чем средняя?

Необходимо исследовать процессы с максимально большими передачами.

Какие использовать пробники?

1. Адроны(анти-) и ядра (наш случай).
2. Электромагнитные пробники (наши соседи).

План

- Вопросы к $p\bar{p}$ взаимодействиям в области $x_T \sim 1$ из исследований pp
- ГНЯР(кумулятивные) в области больших p_T как зонды при исследовании холодной плотной ядерной материи

The first exploration of subatomic structure, by Rutherford, used Au atoms as targets and α particles as *probes*

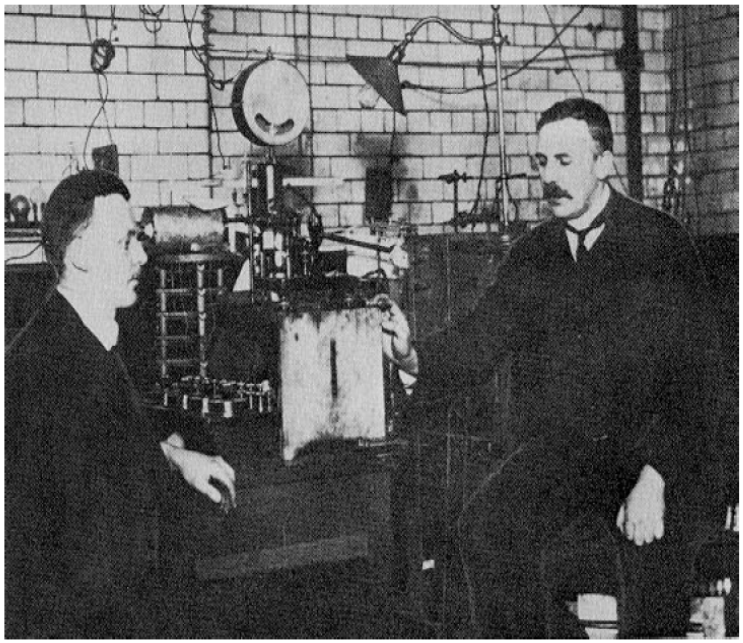

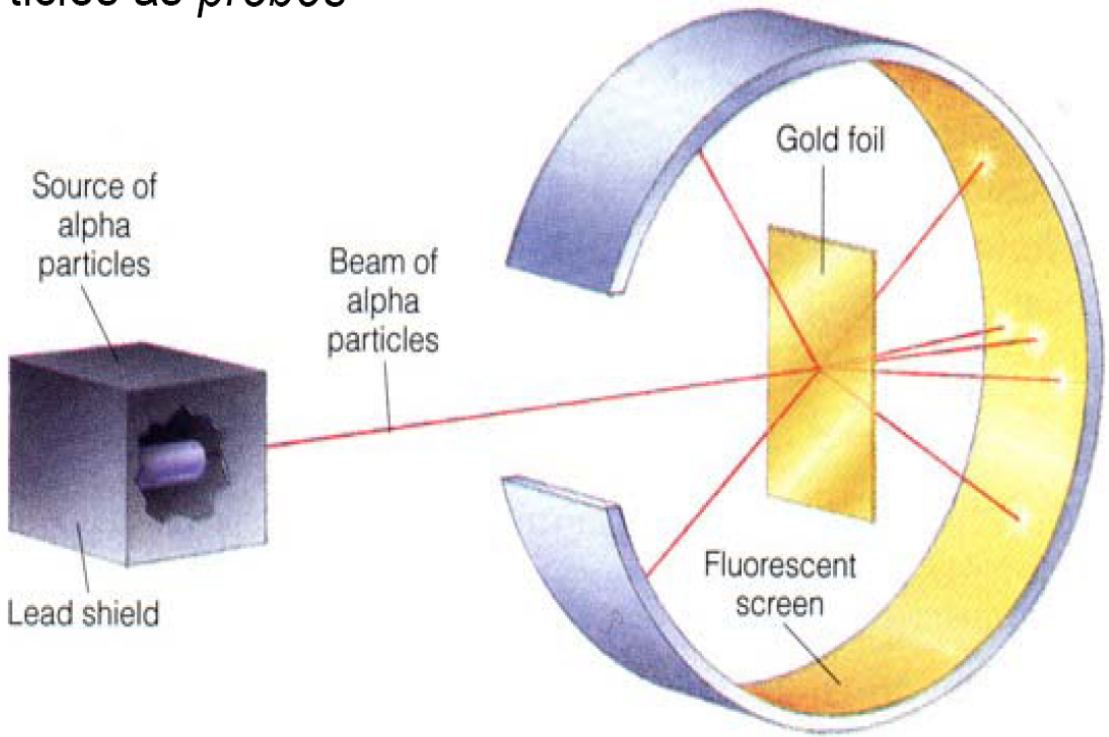

<u>Interpretation:</u>

Positive charge is concentrated in a tiny volume with respect to the atomic dimensions

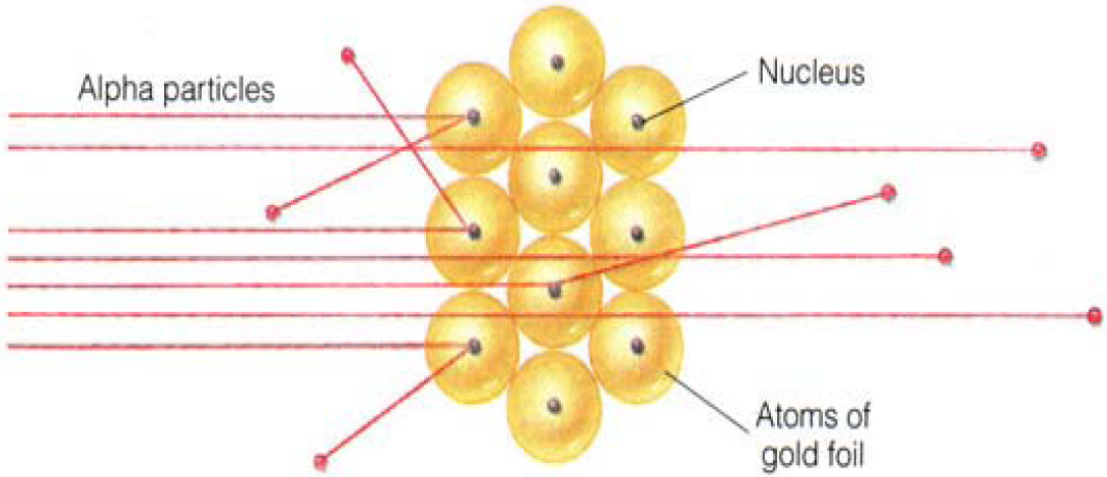

Seeing what the nucleons are made of

The deep inelastic scattering experiments made at SLAC in the 1960s established the quark-parton model and our modern view of particle physics

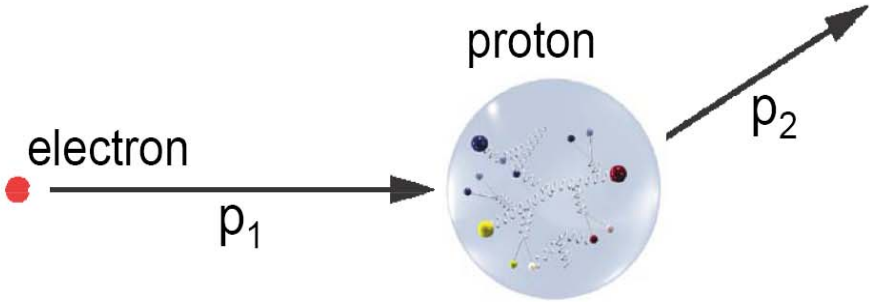

The angular distribution of the scattered electrons reflects the distribution of charge inside the proton

⇒ protons have point-like constituents
⇒ quarks

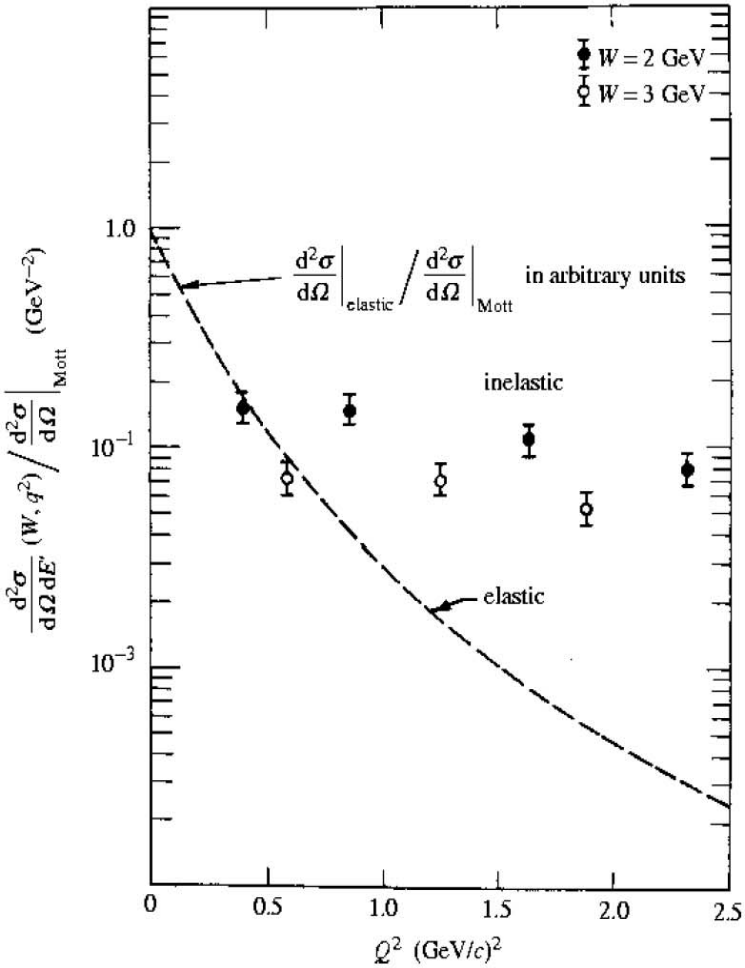

Spin Correlations, QCD Color Transparency, and Heavy-Quark Thresholds in Proton-Proton Scattering

Stanley J. Brodsky and Guy F. de Teramond
Stanford Linear Accelerator Center, Stanford University, Stanford, California 94305
(Received 14 January 1988)

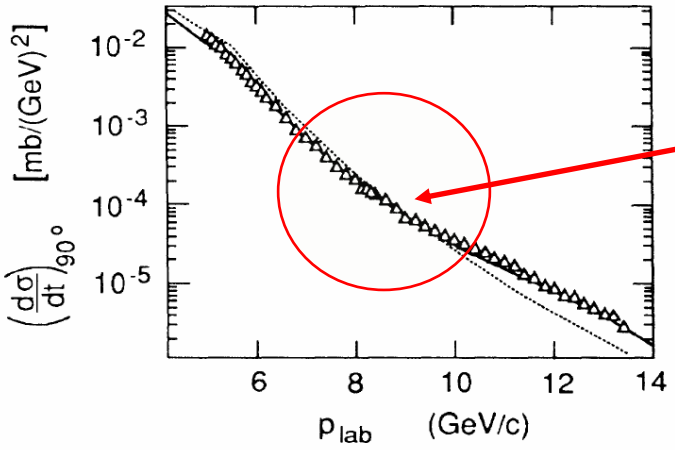

$p_T \sim 2$ GeV/c

FIG. 1. Prediction (solid curve) for $d\sigma/dt$ compared with the data of Akerlof *et al.* (Ref. 16). The dotted line is the background PQCD prediction.

[16]K. Abe *et al.*, Phys. Rev. D **12**, 1 (1975), and references therein. The high-energy data for $d\sigma/dt$ at $\theta_{c.m.} = \pi/2$ are from C. W. Akerlof *et al.*, Phys. Rev. **159**, 1138 (1967); G. Cocconi *et al.*, Phys. Rev. Lett. **11**, 499 (1963); J. V. Allaby *et al.*, Phys. Lett. **23**, 389 (1966).

Comparison of 20 exclusive reactions at large t

C. White,[4,*] R. Appel,[1,5,†] D. S. Barton,[1] G. Bunce,[1] A. S. Carroll,[1]
H. Courant,[4] G. Fang,[4,‡] S. Gushue,[1] K. J. Heller,[4] S. Heppelmann,[2]
K. Johns,[4,§] M. Kmit,[1,‖] D. I. Lowenstein,[1] X. Ma,[3] Y. I. Makdisi,[1]
M. L. Marshak,[4] J. J. Russell,[3]
and M. Shupe[4,§]

TABLE IV. Cross sections at 90 degrees and 5.9 GeV/c incident beam momentum. Reaction number refers to Fig. 27. The values represent interpolations where the range spans 90°.

Number	Reaction	Cross section [nb/(GeV/c)^2]
1	$\pi^+ p \to p\pi^+$	132 ± 10
2	$\pi^- p \to p\pi^-$	73 ± 5
3	$K^+ p \to pK^+$	219 ± 30
4	$K^- p \to pK^-$	18 ± 6
5	$\pi^+ p \to p\rho^+$	214 ± 30
6	$\pi^- p \to p\rho^-$	99 ± 13
7	$K^+ p \to pK^{*+}$	$291 + 47 - 130$
8	$K^- p \to pK^{*-}$	$15 + 10 - 13$
9	$K^- p \to \pi^- \Sigma^+$	50 ± 21
10	$K^- p \to \pi^+ \Sigma^-$	4 ± 3
11	$K^- p \to \Lambda\pi^0$	< 80
12	$\pi^- p \to \Lambda K^0$	< 5
13	$\pi^+ p \to \pi^+ \Delta^+$	45 ± 10
14	$\pi^- p \to \pi^- \Delta^+$	20 ± 11
15	$\pi^- p \to \pi^+ \Delta^-$	24 ± 5
16	$K^+ p \to K^+ \Delta^+$	< 230
17	$pp \to pp$	3300 ± 40
18	$\bar{p}p \to p\bar{p}$	75 ± 8
19	$\bar{p}p \to \pi^+ \pi^-$	7 ± 3
20	$\bar{p}p \to K^+ K^-$	2 ± 2

TABLE V. The scaling between E755 and E838 has been measured for eight meson-baryon and 2 baryon-baryon interactions at $\theta_{\text{c.m.}} = 90°$. The nominal beam momentum was 5.9 GeV/c and 9.9 GeV/c for E838 and E755, respectively. There is also an overall systematic error of $\Delta n_{\text{syst}} = \pm 0.3$ from systematic errors of $\pm 13\%$ for E838 and $\pm 9\%$ for E755.

		Cross section		n-2
No.	Interaction	E838	E755	$(\frac{d\sigma}{dt} \sim 1/s^{n-2})$
1	$\pi^+ p \to p\pi^+$	132 ± 10	4.6 ± 0.3	6.7 ± 0.2
2	$\pi^- p \to p\pi^-$	73 ± 5	1.7 ± 0.2	7.5 ± 0.3
3	$K^+ p \to pK^+$	219 ± 30	3.4 ± 1.4	$8.3^{+0.6}_{-1.0}$
4	$K^- p \to pK^-$	18 ± 6	0.9 ± 0.9	≥ 3.9
5	$\pi^+ p \to p\rho^+$	214 ± 30	3.4 ± 0.7	8.3 ± 0.5
6	$\pi^- p \to p\rho^-$	99 ± 13	1.3 ± 0.6	8.7 ± 1.0
13	$\pi^+ p \to \pi^+ \Delta^+$	45 ± 10	2.0 ± 0.6	6.2 ± 0.8
15	$\pi^- p \to \pi^+ \Delta^-$	24 ± 5	< 0.12	> 10.1
17	$pp \to pp$	3300 ± 40	48 ± 5	9.1 ± 0.2
18	$\bar{p}p \to p\bar{p}$	75 ± 8	≤ 2.1	≥ 7.5

Современные теоретические модели не могут дать количественных предсказаний для эксклюзивных (полуэксклюзивных) процессов. А значит, надо искать возможность разобраться с особенностями структуры ядер(нуклонов) и взаимодействия, используя феноменологию.

Надо работать в области предельной кинематики, аналогия с пороговой кинематикой. В области предельно больших p_T работают валентные составляющие!

Есть ли хорошая модель (феноменологическая) для описания процессов при предельно больших p_T и что она может сказать о структуре взаимодействующих объектов?

Правила кваркового счета (ПКС).

Правилам кваркового счета

Matveev V.A., Muradyan R.M., Tavkhelidze A.N.
Lett. Nuovo Cimento ***7,719 (1973);***

Brodsky S., Farrar G. Phys. Rev. Lett. ***31,1153 (1973)***

Предсказывалось, что для $p_{пучка} \geq 5$ ГэВ/с и углов $\theta_{см} > 40^{o}$

$$\left(\frac{d\sigma}{dt}\right)_{A+B->C+D} \sim s^{-(n_A+n_B+n_C+n_D-2)} f\left(\frac{t}{s}\right)$$

Здесь n_A, n_B, n_C и n_D число валентных кварков в адронах A, B, C и D.

$s=(P_A+P_B)^2$ и $t=(P_A-P_C)^2$,

где P_X – четырех-импульсы адронов.

Например:

$$\left(\frac{d\sigma}{dt}\right)_{pp->pp} \sim s^{-10}$$

и

$$\left(\frac{d\sigma}{dt}\right)_{\pi p->\pi p} \sim s^{-8}$$

Unified description of inclusive and exclusive reactions at all momentum transfers*

R. Blankenbecler and S. J. Brodsky

$$E\frac{d\sigma}{d^3p}(A+B\to C+X)\to(p_T^2)^{-N}f\left(\frac{\mathfrak{M}^2}{s},\frac{t}{s}\right)$$

and[5,6]

$$\frac{d\sigma}{dt}(A+B\to C+D)\to(p_T^2)^{-N}f\left(\frac{t}{s}\right)$$

The entire kinematic range of high-energy inclusive reactions is illustrated on the Peyrou plot of Fig. 1. As usual we define

$$s=(p_A+p_B)^2,\quad t=(p_A-p_C)^2,$$

$$u=(p_B-p_C)^2,\quad \mathfrak{M}^2=(p_A+p_B-p_C)^2,$$

and

$$\epsilon=\mathfrak{M}^2/s\cong(1-p_{\text{c.m.}}/p_{\max}),$$

$$x_T=p_T/p_{\max},\quad x_L=p_L/p_{\max}\simeq(t-u)/s.$$

TABLE I. The expected dominant subprocesses for selected hadronic inclusive reactions at large transverse momentum. The second column lists the important exclusive processes which contribute to each inclusive cross section at $\epsilon\sim 0$. The basic subprocesses expected in the CIM, and the resulting form of the inclusive cross section $Ed\sigma/d^3p\sim(p_\perp{}^2)^{-N}\epsilon^P$ for $p_\perp{}^2\sim\infty$, $\epsilon\to 0$, and fixed $\theta_{\text{c.m.}}$ are given in the last columns. The subprocesses that have the dominant $p_\perp$ dependence at fixed ϵ are underlined. For some particular final-state quantum numbers, the above powers of ϵ should be increased.

Inclusive process	Exclusive-limit channel	Subprocesses	$\frac{d\sigma}{d^3p/E}$ $(\theta\sim 90°)$
$M+B\to M+X$	$M+B\to M+B^*$ $(n=10)$	$\underline{M+q\to M+q}$	$(p_\perp{}^2)^{-4}\epsilon^3$
		$\underline{\bar q+B\to M+qq}$	$(p_\perp{}^2)^{-6}\epsilon^1$
		$M+B\to M+B^*$	$(p_\perp{}^2)^{-8}\epsilon^{-1}$
$B+B\to B+X$	$B+B\to B+B^*$ $(n=12)$	$\underline{B+q\to B+q}$	$(p_\perp{}^2)^{-6}\epsilon^3$
		$\underline{(qq)+(qq)\to B+q}$	$(p_\perp{}^2)^{-6}\epsilon^3$
		$\underline{B+(qq)\to B+qq}$	$(p_\perp{}^2)^{-8}\epsilon^1$
		$B+B\to B+B^*$	$(p_\perp{}^2)^{-10}\epsilon^{-1}$
	$B+B\to B+B^*+M^*$ $(n=14)$	$\underline{q+q\to B+\bar q}$	$(p_\perp{}^2)^{-4}\epsilon^7$
		$q+(qq)\to B+M^*$	$(p_\perp{}^2)^{-6}\epsilon^5$
		$(qq)+B\to B+M^*+qq$	$(p_\perp{}^2)^{-10}\epsilon^1$
		$B+B\to B+B^*+M^*$	$(p_\perp{}^2)^{-12}\epsilon^{-1}$
$B+B\to M+X$	$B+B\to M+B^*+B^*$ $(n=14)$	$\underline{q+(qq)\to M+B^*}$	$(p_\perp{}^2)^{-6}\epsilon^5$
		$q+B\to q(\to M+q)+B^*$	$(p_\perp{}^2)^{-6}\epsilon^5$
		$q+B\to M+q+B^*$	$(p_\perp{}^2)^{-8}\epsilon^3$
		$(qq)+B\to M+B^*+qq$	$(p_\perp{}^2)^{-10}\epsilon^1$
		$B+B\to M+B^*+B^*$	$(p_\perp{}^2)^{-12}\epsilon^{-1}$
	$B+B\to M+M^*+B^*+B^*$ $(n=16)$	$\underline{M+q\to M+q}$	$(p_\perp{}^2)^{-4}\epsilon^9$
		$q+q\to\bar q(\to M+\bar q)+B^*$	$(p_\perp{}^2)^{-4}\epsilon^9$
		$q+q\to M+B^*+\bar q$	$(p_\perp{}^2)^{-6}\epsilon^7$
		$M+B\to M+B^*$	$(p_\perp{}^2)^{-8}\epsilon^5$
	$B+B\to M+M^*+M^*+B^*+B^*$ $(n=18)$	$\underline{q+\bar q\to M+M^*}$	$(p_\perp{}^2)^{-4}\epsilon^{11}$
		$\underline{q+M\to q(\to M+q)+M^*}$	$(p_\perp{}^2)^{-4}\epsilon^{11}$
$B+B\to\bar B+X$	$B+B\to\bar B+B^*+B^*+\overline{B^*}$ $(n=18)$	$\underline{q+q\to B^*+\bar q(\to\bar B+qq)}$	$(p_\perp{}^2)^{-4}\epsilon^{11}$
		$q+q\to B^*+\bar B+qq$	$(p_\perp{}^2)^{-8}\epsilon^7$
		$q+(qq)\to\bar B+B^*+B^*$	$(p_\perp{}^2)^{-10}\epsilon^5$

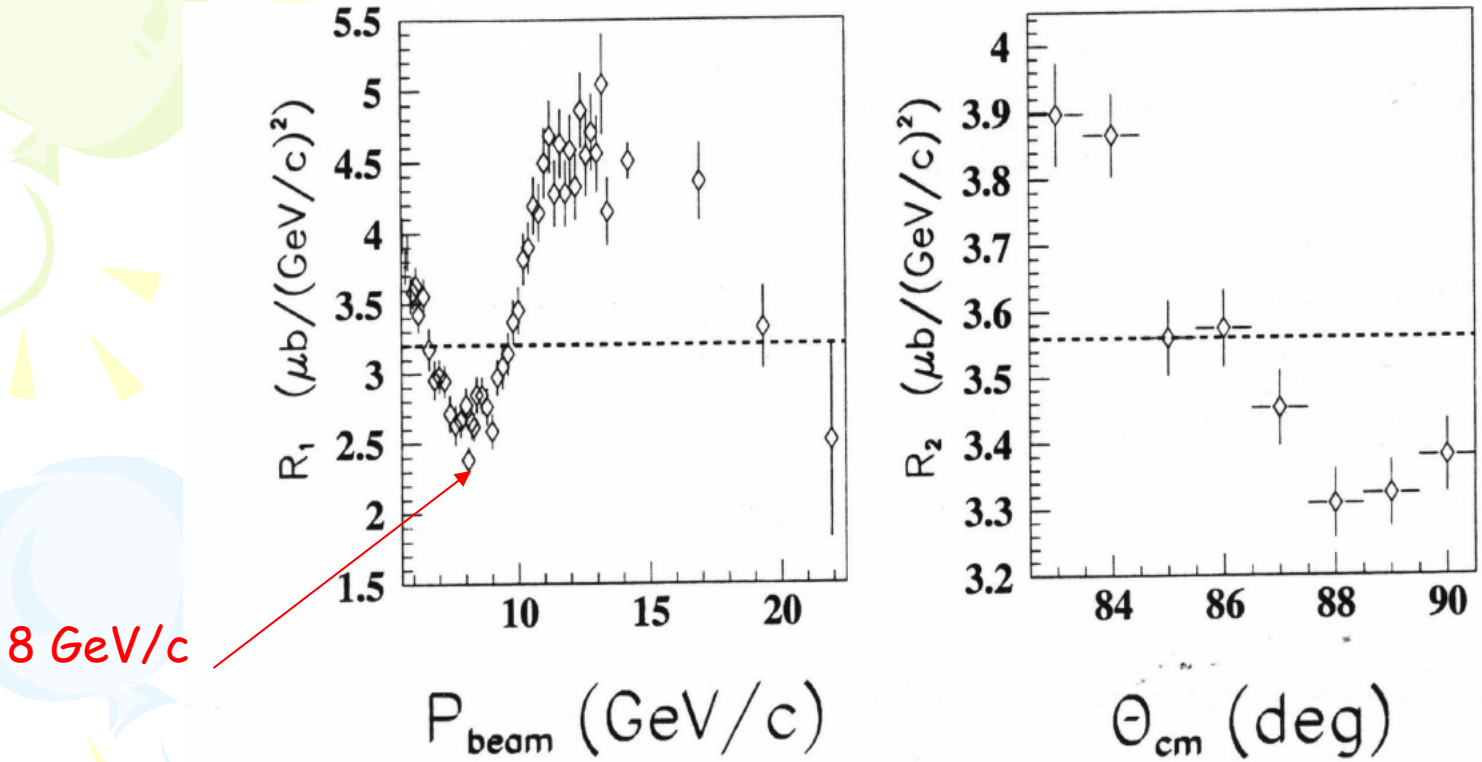

Figure 1.2: Scaled $pp \to pp$ differential cross sections. The dashed lines represent perfect scaling. Their vertical position is arbitrary. **Left** - $R_1 = ((\frac{s}{s_0})^{10} \frac{d\sigma}{dt}(pp))^{-1}$ $(s_0 = 13\ GeV^2)$ at $\theta_{cm} = 90^0$ versus incoming momentum. Data are from Ref. [19]. **Right** - $R_2 = (1 - \cos^2\theta_{cm})^{4\gamma} \frac{d\sigma}{dt}(pp)$ $(\gamma = 1.6)$ at $p_{lab} = 5.9$ GeV/c versus θ_{cm}. Data are from Ref. [17].

Light-Front QCD*

Stanley J. Brodsky

SLAC–PUB–10871
November 2004

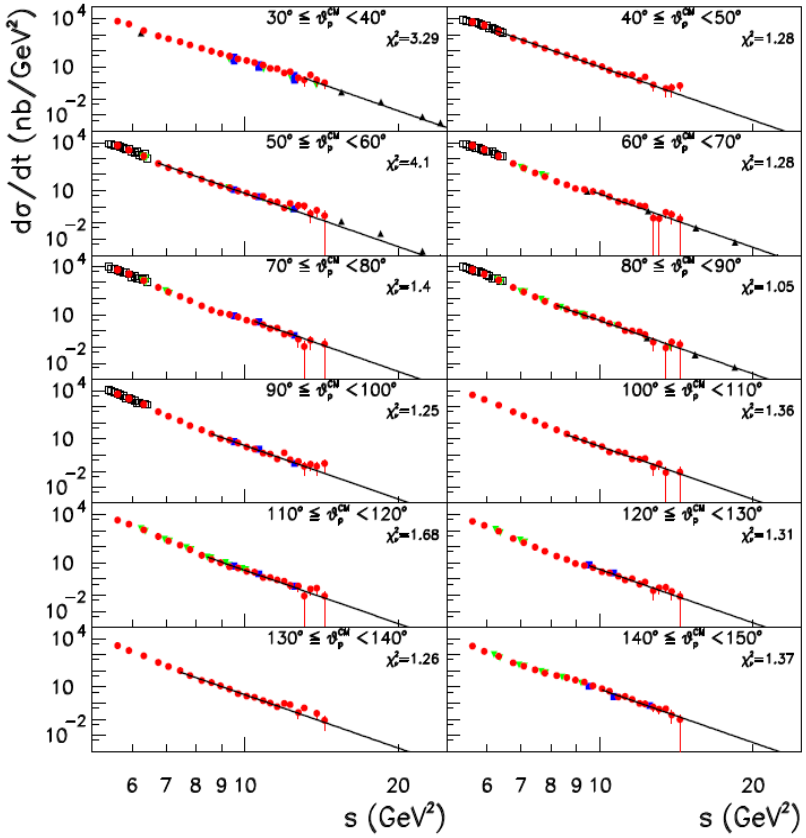

$$s^{11}\frac{d\sigma}{dt}(\gamma d \to pn) \sim$$

constant at fixed CM angle

Figure 8: Fits of the cross sections $d\sigma/dt$ to s^{-11} for $P_T \geq P_T^{th}$ and proton angles between 30° and 150° (solid lines). Data are from CLAS (full/red circles), Mainz(open/black squares), SLAC (full-down/green triangles), JLab Hall A (full/blue squares) and Hall C (full-up/black triangles). Also shown in each panel is the χ^2_ν value of the fit. From Ref. [160].

Pis'ma v ZhETF, vol. 81, iss. 7, pp. 387 – 390 © 2005 April 10

Indication of asymptotic scaling in the reactions $dd \to p^3\mathrm{H}$, $dd \to n^3\mathrm{He}$ and $pd \to pd$

Yu. N. Uzikov[1)]

Joint Institute for Nuclear Research, LNP, 141980 Dubna, Moscow region, Russia

Submitted 11 January 2005

Resubmitted 28 February 2005

It is shown that the differential cross sections of the reactions $dd \to n^3\mathrm{He}$ and $dd \to p^3\mathrm{H}$ measured at c.m.s. scattering angle $\theta_{cm} = 60^\circ$ in the interval of the deuteron beam energy 0.5–1.2 GeV demonstrate the scaling behaviour, $d\sigma/dt \sim s^{-22}$, which follows from constituent quark counting rules. It is found also that the differential cross section of the elastic $dp \to dp$ scattering at $\theta_{cm} = 125-135^\circ$ follows the scaling regime $\sim s^{-16}$ at beam energies 0.5–5 GeV. These data are parameterized here using the Reggeon exchange.

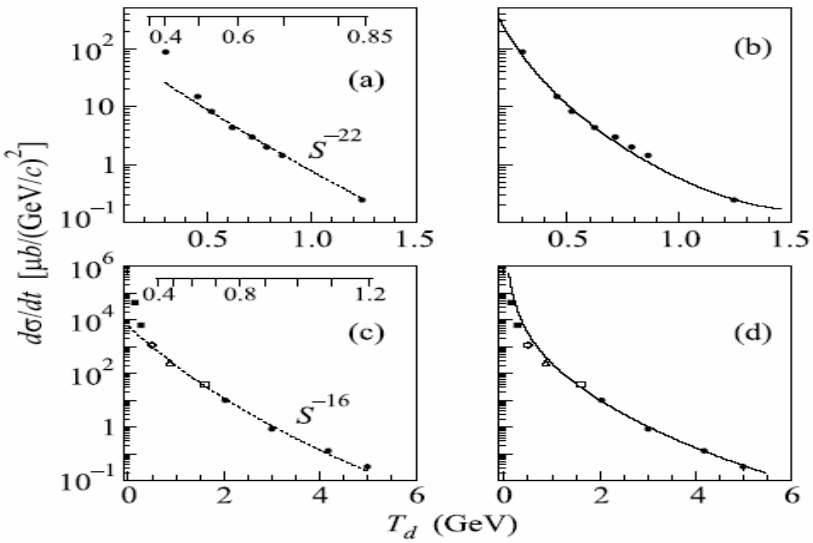

Fig.2. The differential cross section of the $dd \to n^3\mathrm{He}$ and $dd \to p^3\mathrm{H}$ reactions at $\theta_{cm} = 60^o$ (a), (b) and $dp \to dp$ at $\theta_{cm} = 127^o$ (c), (d) versus the deuteron beam kinetic energy. Experimental data in (a), (b) are taken from [20]. In (c), (d), the experimental data (black squares),(○), (△), (open square) and (•) are taken from [22 – 26], respectively. The dashed curves give the s^{-22} (a) and s^{-16} (c) behaviour. The full curves show the result of calculations using Regge formalism given by Eqs. (2), (3), (4) with the following parameters: (b) – $C_1 = 1.9\,\mathrm{GeV}^2$, $R_1^2 = 0.2\,\mathrm{GeV}^{-2}$, $C_2 = 3.5$, $R_2^2 = -0.1\,\mathrm{GeV}^{-2}$; (d) – $C_1 = 7.2\,\mathrm{GeV}^2$, $R_1^2 = 0.5\,\mathrm{GeV}^{-2}$, $C_2 = 1.8$, $R_2^2 = -0.1\,\mathrm{GeV}^{-2}$. The upper scales in (a) and (c) show the relative momentum q_{pn} (GeV/c) in the deuteron for the ONE mechanism

Energy dependence of spin-spin effects in p-p elastic scattering at 90°$_{c.m.}$

E. A. Crosbie, L. G. Ratner, and P. F. Schultz
Argonne National Laboratory, Argonne, Illinois 60439

J. R. O'Fallon
Argonne Universities Association, Argonne, Illinois 60439

D. G. Crabb, R. C. Fernow,* P. H. Hansen,† A. D. Krisch, A. J. Salthouse,‡ B. Sandler,§ T. Shima, and K. M. Terwilliger
Randall Laboratory of Physics, The University of Michigan, Ann Arbor, Michigan 48109

N. L. Karmakar
University of Kiel, Kiel, Germany

S. L. Linn‖ and A. Perlmutter
Department of Physics and Center for Theoretical Studies, The University of Miami, Coral Gables, Florida 33124

P. Kyberd
Nuclear Physics Laboratory, Oxford University, Oxford, England
(Received 31 March 1980)

The energy dependence of the spin-parallel and spin-antiparallel cross sections for $p_\uparrow + p_\uparrow \to p + p$ at 90°$_{c.m.}$ was measured for beam momenta between 6 and 12.75 GeV/c. The ratio $(d\sigma/dt)_{\text{parallel}}$:$(d\sigma/dt)_{\text{antiparallel}}$ at 90° is about 1.2 up to 8 GeV/c and then increases rapidly to a value of almost 4 near 11 GeV/c. Our data indicate that this ratio may depend only on the variable $P_\perp{}^2$, and suggests that the ratio may reach a limiting value of about 4 for large $P_\perp{}^2$.

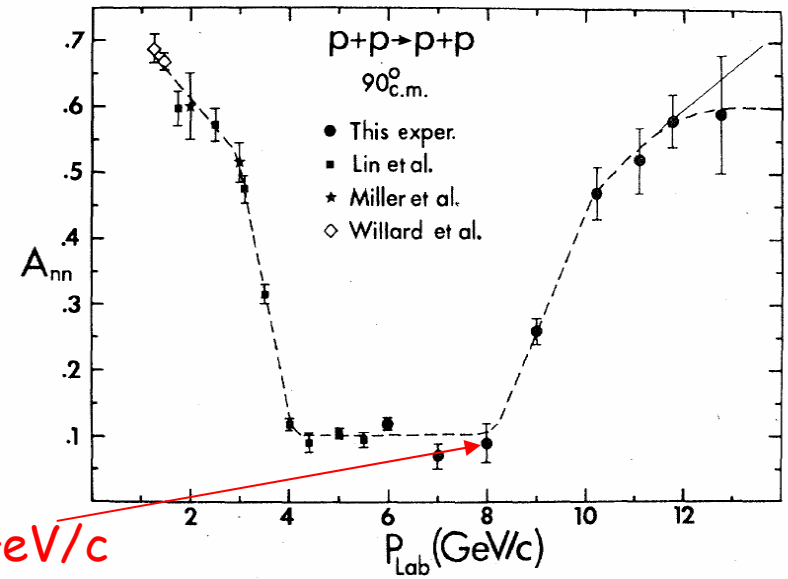

FIG. 2. Plot of the spin-spin correlation parameter A_{nn} for $p+p \to p+p$ at 90°$_{c.m.}$ as a function of incident beam momentum. The dashed and solid lines are hand-drawn possible fits.

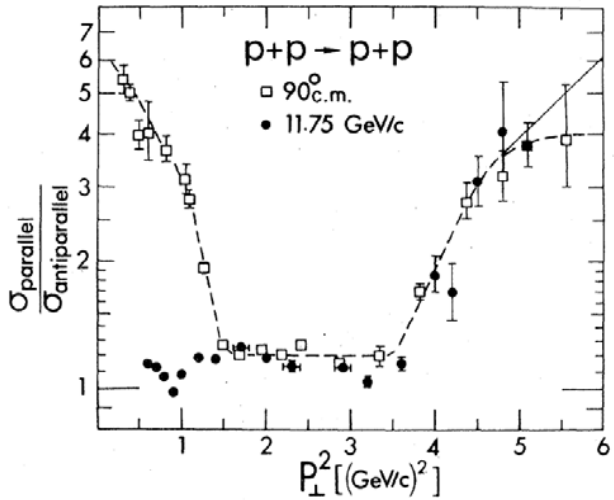

FIG. 3. Plot of the ratio of the spin-parallel to spin-antiparallel differential cross sections, as a function of $P_\perp{}^2$, for p-p elastic scattering. The squares are the fixed-angle data at 90°$_{c.m.}$, with the incident energy varied. The circles are data (Refs. 5, 11) with the momentum held fixed at 11.75 GeV/c while the scattering angle is varied. The dashed and solid lines are hand-drawn possible fits to the 90°$_{c.m.}$ data.

Shimanskiy S.S.

QCD with and in nuclei: color transparency and short-range correlations in nuclei - theory, observations, directions for further studies

Mark Strikman
104 Davey Lab, Penn State University, University Park, PA 16802, USA

arXiv:0903.1941v2 [hep-ph] 2 Apr 2009

Совещание PANDA март 2009

Abstract

We summarize basic theoretical ideas which let to the observation of the short-range correlations (SRC) in nuclei using hard probes and outline directions for probing quark-gluon structure of SRCs. Implications of the observations of color transparency for processes involving pions are reviewed. Open questions and directions for further studies of color transparency phenomena using hadronic projectiles are presented using as an example the PANDA detector at FAIR.

Key words: short-range correlations, color transparency
PACS: 25.30.-c, 25.40.-h, 24.85.+p

Farrar has expressed meson-baryon scattering amplitudes as a sum of terms involving valence quark scattering amplitudes [17]. The amplitudes can be subdivided into four basic categories, shown in Fig. 1, which are described by pure gluon exchange (GEX), quark interchange (INT) between the hadrons, quark-antiquark annihilation (ANN) and pair creation, or a combination (COMB) of the above. The quark scattering amplitudes

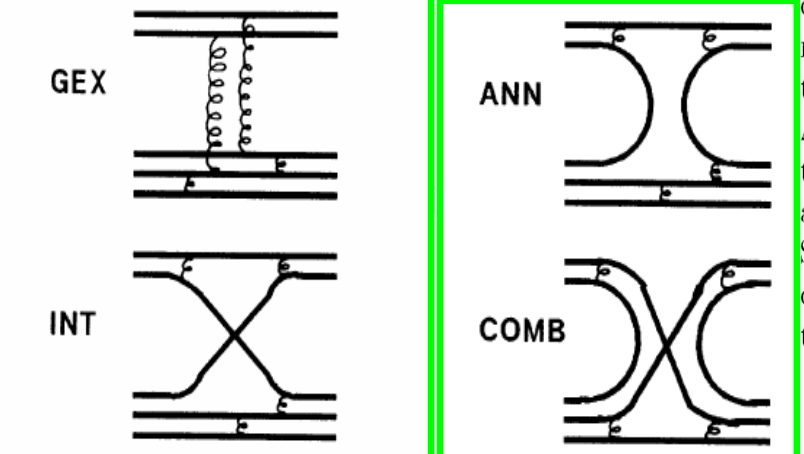

i. Study of the two body processes large angle processes with nucleon targets

Understanding of the large angle exclusive processes: $a + b \to c + d$ remains one of the challenges for pQCD. Systematic study of a large variety of reactions is available only for incident momentum of 6 and 9.9 GeV/c and below [27]. Analysis [27] found that cross sections of the processes where quark exchanges are allowed are much larger, and the energy dependence is roughly consistent with quark counting rules. Among the biggest puzzles is the ratio of $\theta_{c.m.} = 90^o$ cross sections of $\bar{p}p$ and pp elastic scattering which is below 4% at 6 GeV/c. At face value, it indicates extremely strong suppression of the diagrams with gluon exchanges in t channel, though more systematic, more precise studies are clearly necessary. Another puzzle is the oscillation of the differential cross section of the elastic pp scattering at large t around a smooth quark counting inspired parametrization. Are these oscillations present in any of the $p\bar{p}$ channels?

It appears that PANDA will have excellent acceptance for numerous large angle processes - from the simplest processes $p\bar{p} \to p\bar{p}, \pi\pi, K\bar{K}$ to the processes of production of multi particle states: baryon - antibaryon and meson pairs, etc. In the case of the proton beam the elastic channel is covered reasonably well, though the channels involving Δ-isobars, nonresonance πN production, etc are practically not known. Another gap in the knowledge is pn scattering which could be studied using the ^{2}H pellets. There is a suggestion that the measurement of the pn/pp ratio may provide an insight on the SU(6) structure of the nucleon wave function at large x [28]. Overall, comparing all these channels in pN and $\bar{p}N$ scattering may lead to a break through in understanding hard two body reactions.

Если ПКС так хорошо связаны с составной структурой взаимодействующих объектов, то мы, исследовав поведение сечений (цветовой прозрачности, кумулятивных процессов), можем въявь обнаружить вклад взаимодействий с многокварковыми объектами.

Что хотим изучать?

Природу аномального поведения сечений и поляризационных характеристик.

Эксклюзивные реакции в области больших p_T неполяризованный и поляризованный пучки.

B (p,Λ, …), M (π, K , e…)

$$p\uparrow + p\uparrow \rightarrow B + B + M\overline{M}$$

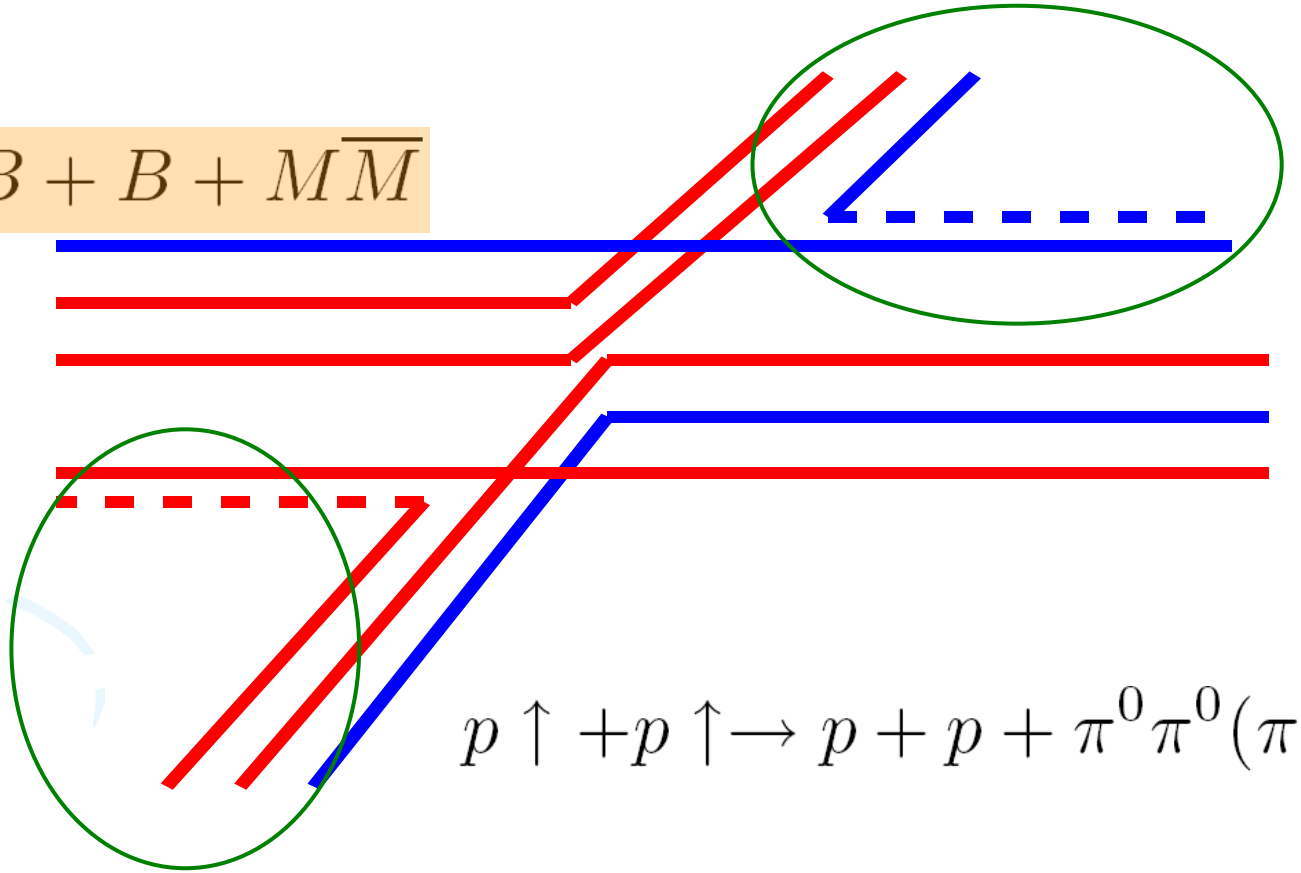

$$p\uparrow + p\uparrow \rightarrow p + p + \pi^0\pi^0(\pi^+\pi^-)$$

Какие характеристики будем смотреть и для чего?

1. «Демократия» во взаимодействии кварков и дикварков.

$$R = \frac{N(\pi^+\pi^-)}{N(\pi^0\pi^0)} = \frac{2}{7}$$

2. Доминирование определенного вида дикварков

$$R = \frac{N(\pi^+\pi^-)}{N(\pi^0\pi^0)} \to 0$$

3. Прохождение областей резонансов эффективной массой пары($\pi\pi \to \rho$, КК $\to\phi$, ...) как изменится R и в каком спиновом состоянии будет пара?

4. Как связаны плоскости pp->pp и pp->MM ? (В случае дикварков – ни как).

5. .....

Поляризованный пучок и/или мишень

1. Анализирующая способность BB -пары. (Для дикваркового механизма «0»).

2. Анализирующая способность MM-пары. (Для дикваркового механизма зависит от вида qq-взаимодействия).

Problems for PANDA

- Elastic $p\bar{p}$ scattering at $x_T \sim 1$ (counting rules violation, $p_T \sim 2$ Gev/c anomaly …);

- Exclusive reactions $\bar{p} + p \to \bar{B}B + \bar{M}M$

  where B – baryons N, Λ, Δ^{B+M} …,

  M – mesons or leptons

  (diquarks, $\bar{q}q$-vertex…).

The knowledge $p\bar{p}$ interactions at $x_T \sim 1$ are necessary to study high p_T DINR !!!

DINR(cumuative) at high p_T as probes of the cold dense nuclear matter

Cumulative processes

SOVIET PHYSICS JETP VOLUME 6 (33), NUMBER 5 MAY, 1958

ON THE FLUCTUATIONS OF NUCLEAR MATTER

D. I. BLOKHINTSEV

Joint Institute for Nuclear Research

Submitted to JETP editor July 1, 1957

J. Exptl. Theoret. Phys. (U.S.S.R.) 33, 1295-1299 (November, 1957)

It is shown that the production of energetic nuclear fragments in collisions with fast nucleons can be interpreted in terms of collisions of the incoming nucleon with the density fluctuations of the nuclear matter.

1. INTRODUCTION

THE motion of nucleons in nuclei can result in short-lived tight nucleon clusters, in other words, in density fluctuations of nuclear matter. Since such clusters are relatively far removed from the other nucleons of the nucleus, they become atomic nuclei of lower mass in a state of fluctuating compression.

In their study of the scattering of 675-Mev protons by light nuclei, Meshcheriakov and coworkers[1,2] observed recently certain effects which confirm the existence of such fluctuations, at least for the simplest nucleon-pair fluctuations, which lead to the formation of a compressed deuteron.

We recall in this connection reports in earlier works[3,4] that high-energy nucleons can split nuclei into "supra-barrier" fragments, i.e., fragments with an energy much larger than their binding energy and the energy of the Coulomb barrier. However, there was a lack of quantitative experimental data on which to base the theoretical analysis.

Some authors related this curious process, without foundation, to hypothetical long-range nuclear forces. Others tried to connect it with nuclear many-body forces.

The experimental data on the emission of high-energy deuterons from light nuclei give support to the idea that "supra-barrier" fragments are produced also by direct collision of an incoming nucleon with a tight nucleon cluster that results from density fluctuations of the nuclear matter. We offer in the following a quantitative argument in favor of the production of fast deuterons and other "supra-barrier" fragments by such fluctuations.

Concerning the nuclear many-body forces, it should be noted that, according to existing estimates,[5] there is no reason to believe that they are considerably stronger than the two-body forces. At the instant of dense clustering both paired and collective interactions may take place. However, at present there exists no experimental information which would allow an explanation of this interaction, or in particular allow a determination of the relative contributions of the paired and the collective interactions.

2. INTERACTION OF DEUTERONS WITH FAST PROTONS

It was shown experimentally[1,2] that scattering of 675-Mev protons by deuterium produces, in addition to scattered nucleons, a small number of undestroyed deuterons of high energy (up to 660 Mev). This shows that in such collisions the nucleon imparts an appreciable fraction of its momentum to the deuteron as a whole.

FLUCTUONS AND HIGH MOMENTUM TRANSFER IN NUCLEAR PROCESSES*

D.I.Blokhintsev, A.V.Efremov, V.K.Lukjanov, A.I.Titov

JINR, Dubna

Abstract

The report summarizes the results of a series of works made recently in JINR, which explore the hypothesis about "fluctuons", i.e. multibaryon configurations of the mass $k\,m$ nucleon and correlation region of an order of elementary particles.

The probability of fluctuon-formation is calculated by the "quark bag" model. It is argued that the cumulative production is due to the hard scattering process (similar to high $p_\perp$ hadron production) of beam particle partons with partons of a fluctuon considered as a hadron made of $3k$ quarks.

The model explains many qualitative and quantitative features of cumulative processes: The yield of cumulative hadrons, polarization of baryons, elastic and deep inelastic ed-scattering and so on. All this gives right to consider the cumulative processes as a new source of information about quark dynamics at small distance.

I. Fluctuons

It is as early as the fifties theoretists became interested in the appearance of "above-barrier fragments /1/. The phenomenon consists in knocking out by protons of light nuclei (fragments) from heavier nuclei when the momentum transferred to a light nucleus is much larger than the binding energy of this nucleus.

At the same time, the hypothesis/2/ has been proposed that a large momentum can be transferred to a complex system of nucleons as a whole only when at the moment of collision with an incident particle a number of internuclear nucleons are inside a small volume, due to quantum fluctuations, and takes the momentum transfer as a unique particle with mass $M_k = km$ (m is the nucleon mass, k the number of nucleons in the group). A multi-nucleon formation of this type has recently been called as a "fluctuon".

1. Adjgirey L.S. et al. JETP, 33 (1957) 1185.
2. Blokhintsev D.I. JETP, 33 (1957) 1295.

* A report submitted to the XIX International Conference on High Energy Physics, Tokyo, 1978.

The first introduction of the term “cumulative effect”

Выражаю глубокую благодарность С. Б. Герасимову, А. Б. Говоркову и Г. Н. Флерову за обсуждение изложенных соображений. Как мне стало известно, Г. Н. Флеров еще несколько лет назад высказывал мысль о возможных кумулятивных эффектах при сооружении релятивистских ядер.

Поступила в редакцию
11 ноября 1970 г.

Литература

E2-85-537

A.V.Efremov, V.T.Kim, G.I.Lykasov

HARD HADRON-NUCLEUS PROCESSES AND MULTIQUARK CONFIGURATIONS IN NUCLEI

V. Conclusion

The analysis of the inclusive large x_1 meson production in the hard hadron processes on nuclei has allowed one to understand the relative contribution of multiple rescattering processes and the existence of multiquark fluctons in the nucleus in dependence on x_1 the multiple rescattering processes are dominating at $x_1 < 0.7 \div 0.8$ whereas at larger x_1 the mechanism of hard scattering on fluctons is dominating. The model of multiple rescattering in which the multiple soft collisions suggested in this paper are taken into account before the hard collision allows one to describe the multiple rescattering processes inside the nucleus correctly.

The flucton model succesfully used earlier for the description of the cumulative production and EMC-effect with such parameters is applied for the description of anomalous phenomena in the large p_1 processes in nuclei.

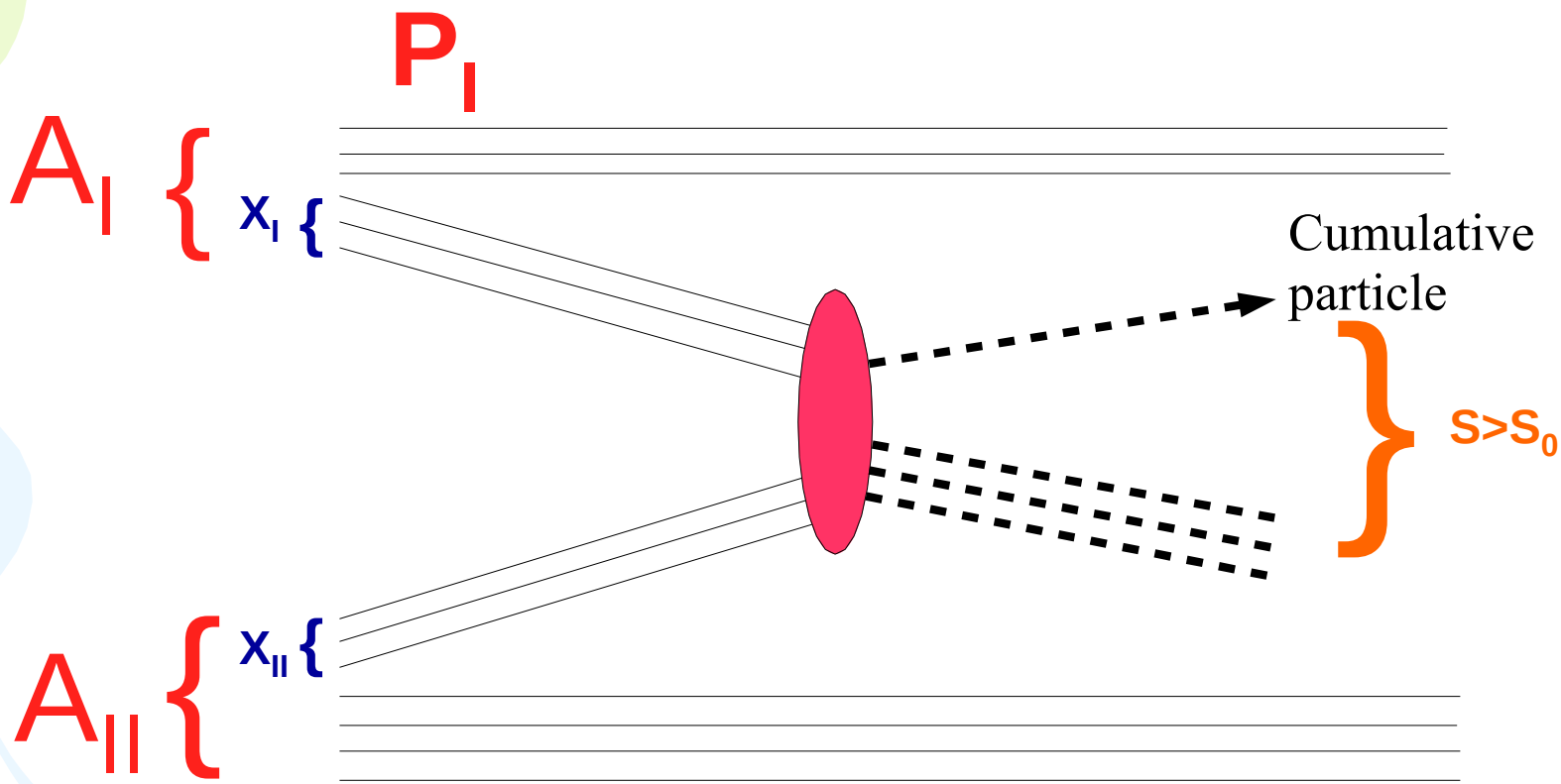

$$s_0 = \left(\frac{\mathbf{P_I}}{\mathbf{A_I}} + \frac{\mathbf{P_{II}}}{\mathbf{A_{II}}}\right)^2$$

kinematics' limit for free NN-interaction

$$s_{cumulative} = (X_I \cdot \frac{P_I}{A_I} + X_{II} \cdot \frac{P_{II}}{A_{II}})^2$$

Cumulative and Subthreshold processes

$$S_{cumulative} > S_0$$

$X_I \in [0, A_I]$ and $X_{II} \in [0, A_{II}]$

$X_I = X_{II} = 1$ - for free NN-interaction kinematical borders

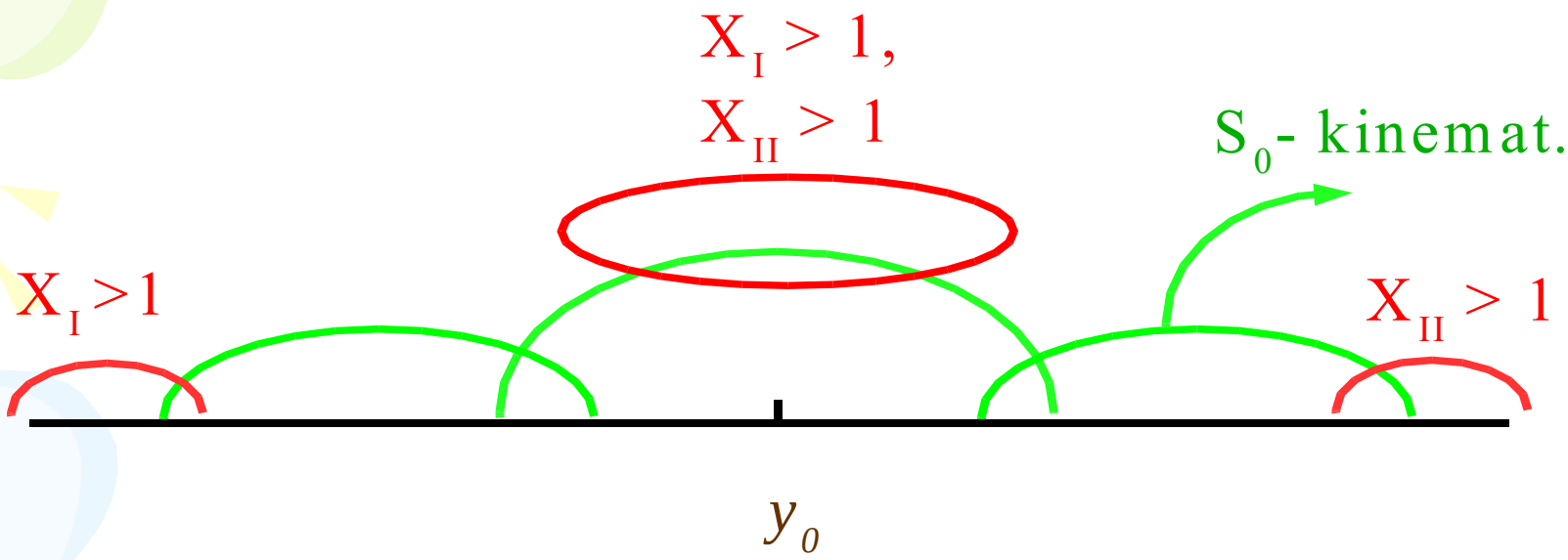

Cumulative processes:

1) $X_I = 1$ and $X_{II} > 1$ } **Fragmentation**
2) $X_{II} = 1$ and $X_I > 1$ } **regions**
3) $X_I > 1$ and $X_{II} > 1$ **Central region**

Fragmentation regions

$\mu + N_{min} \cdot m \rightarrow m_c + [N_{min} \cdot m + \Delta]$

for $E_\mu >> m_i , E_c$

$$X = N_{\min} = Q \cong \frac{(E_c - \beta_\mu \cdot P_c \cdot \cos\theta_c)}{m} + \ldots \equiv X_I (X_{II})$$ **Stavinsky (1970's)**

Common case for AA-collisions

V.S. Stavinsky JINR Rapid Communications N18-86, p.5 (1986)

$(X_I \cdot M_I) + (X_{II} \cdot M_{II}) \rightarrow m_c + [X_I \cdot M_I + X_{II} \cdot M_{II} + m_2]$

$$S_{\min}^{1/2} = \min(S^{1/2}) = \min[(X_I \cdot P_I + X_{\mathrm{II}} \cdot P_{II})^{1/2}]$$

Рассмотрим квазибинарное столкновение в виде масс сталкивающихся объектов:

$$X_I \cdot M_I + X_{II} \cdot M_{II} \quad \rightarrow \quad M_c \ + (X_I \cdot M_I + X_{II} \cdot M_{II} + M_\Delta).$$

В случае столкновения ядер $X_I \in [0, A_I]$ и $X_{II} \in [0, A_{II}]$, где A_I и A_{II} атомные веса ядер I и II соответственно. В случае, если I или II адрон тогда соответствующая переменная $X \in [0, 1]$. Для ядер $M_I = M_{II} = m_N$, где m_N масса нуклона. M_Δ - масса компенсирующая выполнение минимальных законов сохранения в квазибинарной реакции. M_c - масса наблюдаемой частицы в кумулятивной области.

Максимальную энергию кумулятивная частица будет иметь когда остальная масса будет как единый объект. Закон сохранения энергии-импульса для такой квазибинарной реакции можно записать в обозначениях 4-х векторов так:

$$X_I \cdot P_I + X_{II} \cdot P_{II} = P_c + P_X.$$

Здесь P_c четырех-импульс кумулятивной частицы, а P_X четырех-импульс компенсирующей массы.

Переносим P_c в левую часть, возводим в квадрат и приводим подобные, после чего получаем соотношение:

$$M_c^2 + 2 \cdot X_I \cdot X_{II} \cdot (P_I \cdot P_{II}) - 2 \cdot X_I \cdot (P_I \cdot P_c) - 2 \cdot X_{II} \cdot (P_{II} \cdot P_c) =$$

$$2 \cdot X_I \cdot X_{II} \cdot (M_I \cdot M_{II}) + 2 \cdot X_I \cdot (M_I \cdot M_\Delta) + 2 \cdot X_{II} \cdot (M_{II} \cdot M_\Delta) + M_\Delta^2.$$

Собираем все члены содержащие X_{II} в левой части и выносим X_{II} в качестве общего множителя получим:

$$2 \cdot X_{II}\{X_I[(P_I \cdot P_{II}) - M_I \cdot M_{II}] - [(P_{II} \cdot P_c) + M_{II} \cdot M_\Delta]\} 2 \cdot X_I[(P_I \cdot P_c) + M_I \cdot M_\Delta] + M_\Delta^2 - M_c^2.$$

Отсюда получаем связь между X_I и X_{II}:

$$X_{II} = \frac{X_I \cdot A + B}{X_I - C}, \tag{1}$$

где

$$A = \frac{[(P_I \cdot P_c) + M_I \cdot M_\Delta]}{[(P_I \cdot P_{II}) - M_I \cdot M_{II}]}, \tag{2}$$

$$B = \frac{M_\Delta^2 - M_c^2}{2 \cdot [(P_I \cdot P_{II}) - M_I \cdot M_{II}]}, \tag{3}$$

$$C = \frac{[(P_{II} \cdot P_c) + M_{II} \cdot M_\Delta]}{[(P_I \cdot P_{II}) - M_I \cdot M_{II}]}. \tag{4}$$

Согласно Ставинскому[1], для определения единственных значений X_I и X_{II} выберем условие, что величина s определенная как:

$$s = (X_I \cdot P_I + X_{II} \cdot P_{II})^2 = (X_I^2 \cdot M_I^2 + X_{II}^2 \cdot M_{II}^2 + 2 \cdot X_I \cdot X_{II}(P_I \cdot P_{II})). \tag{5}$$

Или в другом виде

$$s = (X_I^2 \cdot M_I^2 + X_{II}^2 \cdot M_{II}^2 + 2 \cdot X_I \cdot X_{II} \cdot D), \tag{6}$$

где

$$D = (P_I \cdot P_{II}). \tag{7}$$

s выраженная как (6) через переменные X_I и X_{II} должна иметь минимальное значение. При этом X_{II} выражается через X_I по формуле (1). A,B,C и D константы даются формулами (2),(3),(4) и (7) соответственно. M_I и M_{II} тоже константы. Можно получить аналитическое решения в общем случае используя пакеты аналитических вычислений (например MATHEMATICA). Пока не видно элегантного выражения, формулы довольно громоздкие.

Легко получить некоторые частные случаи, когда не нужно делать минимизацию.

1. Классический кумулятивный эффект $p + A \to c + X (X_I = 1)$.

$$X_{II} = \frac{A + B}{1 - C}. \tag{8}$$

2. Подпороговое рождение, дважды кумулятивные процессы ($X_I = X_{II}$).

$$X_I = X_{II} = \frac{C + A}{2} \pm \sqrt{\frac{(C + A)^2}{4} + B}. \tag{9}$$

Ссылки

[1] V.S. Stavinsky, JINR Rapid Commun. **N18-86**, p.5, 1986.

A.A. Baldin's parameterization

Phys. At. Nucl. 56(3), p.385(1993)

$$\Pi = \frac{1}{2}(X_I^2 + X_{II}^2 + 2 \cdot X_I \cdot X_{II} \cdot \gamma_{I,II})^{\frac{1}{2}} = \frac{1}{2 \cdot m} \cdot S_{\min}^{\frac{1}{2}}$$

$$\gamma_{I,II} = \frac{(P_I \cdot P_{II})}{M_I \cdot M_{II}}$$

Inclusive data parameterization

$$E \cdot \frac{d^3\sigma}{dp^3} = C_1 \cdot A_I^{\frac{1}{3}+\frac{X_I}{3}} \cdot A_{II}^{\frac{1}{3}+\frac{X_{II}}{3}} \cdot \exp(-\frac{\Pi}{C_2}),$$

$$C_1 = 2200[mb \cdot GeV^{-2} \cdot c^3 \cdot sr^{-1}], C_2 = 0.127$$

A.A. Baldin's parameterization for cumulative and subthreshold particle production

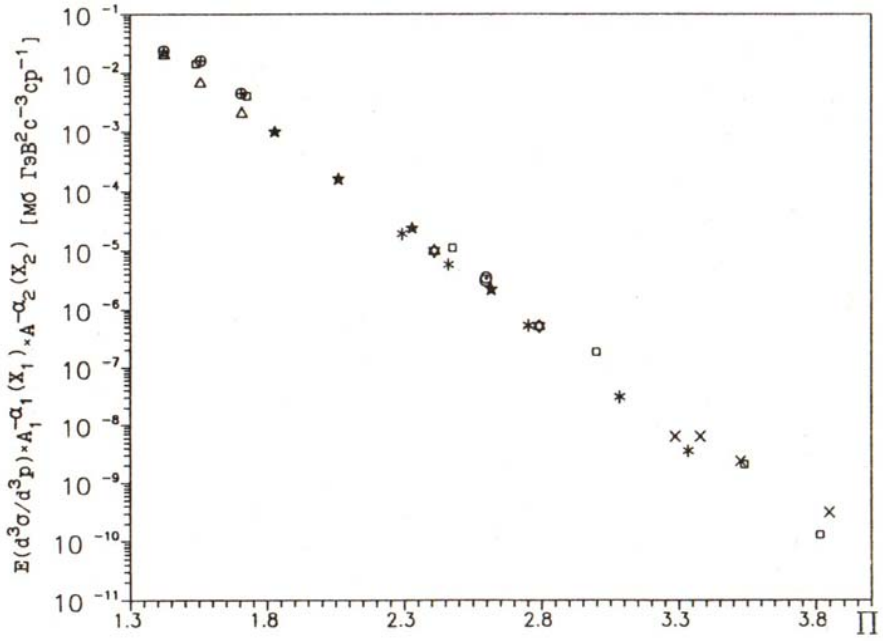

Рис.1. Зависимость инвариантных дифференциальных сечений, деленных на $A^{\alpha_1(X_1)}A^{\alpha_2(X_2)}$, где $\alpha_1(X_1) = 2/3 + X_1/3$ и $\alpha_2(X_2) = 2/3 + X_2/3$, от параметра П для следующих реакций: * Si + Si → K^- 2,0 ГэВ/нуклон, 0°[9]; × Si + Si → $\bar{p}$ 2,0 ГэВ/нуклон, 0°[9]; ✡ Si + Si → K^- 1,4 ГэВ/нуклон, 0°[8] o C + C → $\bar{p}$ 3,65 ГэВ/нуклон, 24°[11]; o d + C → $\bar{p}$ 3,65 ГэВ/нуклон, 24°[11]; ⊕ C + C → K^- 2,5—3,65 ГэВ/нуклон, 24°[12]; Δ d + C → K^- 2,5—3,65 ГэВ/нуклон, 24°[12]; ⋆ p + C → K^- 9,2 ГэВ/нуклон, 119°[6]; □ p + C → π^- 9,2 ГэВ/нуклон, 119°[7]

Реакция	Екин. ГэВ/н	Лаб. имп. ГэВ/с	Лаб. угол вылет	$\sigma_{экс}=\frac{E}{p^2}\times\frac{d^2\sigma}{dp\times d\Omega}$ мб/ср ГэВ^2/с^3	$\sigma_{рас}=\frac{E}{p^2}\times\frac{d^2\sigma}{dp\times d\Omega}$ мб/ср ГэВ^2/с^3	Ссылка
d+C ->$\bar{p}$	3.65	0.8	24^0	$(1.5\pm0.6)\times10^{-4}$	9.3×10^{-5}	11
C+C ->$\bar{p}$	3.65	0.8	24^0	$(1.2\pm0.3)\times10^{-3}$	7.4×10^{-4}	11
C+Cu->$\bar{p}$	3.65	0.8	24^0	$(6.2\pm2.0)\times10^{-3}$	6.05×10^{-3}	11
Si+Si->$\bar{p}$	2.0	1.0	0^0	$(8.71\pm2.9)\times10^{-5}$	1.98×10^{-4}	9
Si+Si->$\bar{p}$	2.0	1.5	0^0	$(1.03\pm0.25)\times10^{-4}$	1.2×10^{-4}	9
Si+Si->$\bar{p}$	2.0	1.9	0^0	$(4.9\pm1.0)\times10^{-5}$	5.07×10^{-5}	9
Si+Si->$\bar{p}$	1.65	1.5	0^0	$(1.41\pm0.38)\times10^{-5}$	9.1×10^{-6}	9
d+C->k^-	2.5	0.8	24^0	$(4.1\pm2.0)\times10^{-2}$	5.7×10^{-2}	12
C+C->k^-	2.5	0.8	24^0	$(4.6\pm1.0)\times10^{-1}$	4.4×10^{-1}	12
Si+Si->k^-	1.0	1.0	0^0	$(1.2\pm1.5)\times10^{-3}$	1.1×10^{-3}	8
Si+Si->k^-	1.26	1.0	0^0	$(8.0\pm5.0)\times10^{-3}$	2.26×10^{-2}	8
Si+Si->k^-	1.4	1.0	0^0	$(5.0\pm1.5)\times10^{-2}$	7.0×10^{-2}	8
Si+Si->k^-	1.4	1.5	0^0	$(5.0\pm1.5)\times10^{-3}$	7.56×10^{-3}	8
Si+Si->k^-	2.0	2.37	0^0	$(1.5\pm1.0)\times10^{-2}$	1.66×10^{-2}	9
Si+Si->k^-	2.0	1.5	0^0	$(2.5\pm0.5)\times10^{-1}$	3.46×10^{-1}	9
Si+Si->k^-	2.0	1.0	0^0	$(1.5\pm0.5)\times10^{-3}$	1.45×10^{0}	9

Cumulative processes.

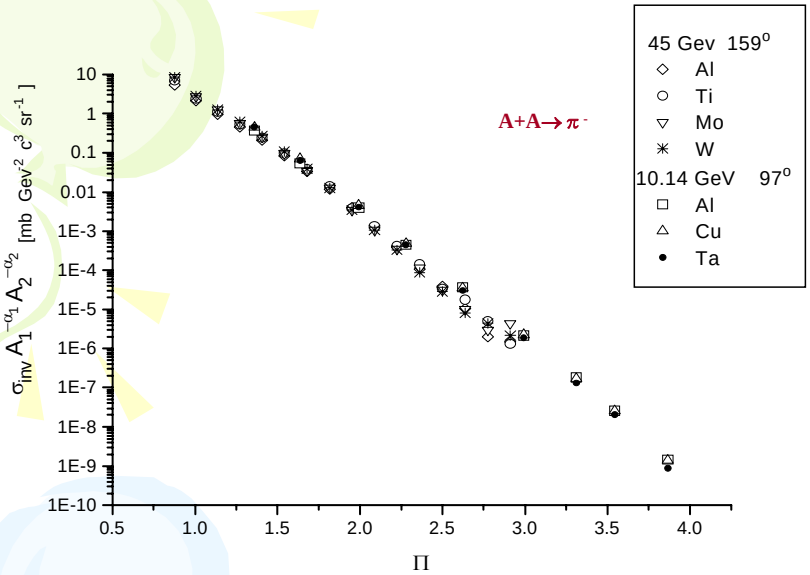

Twice cumulative processes.

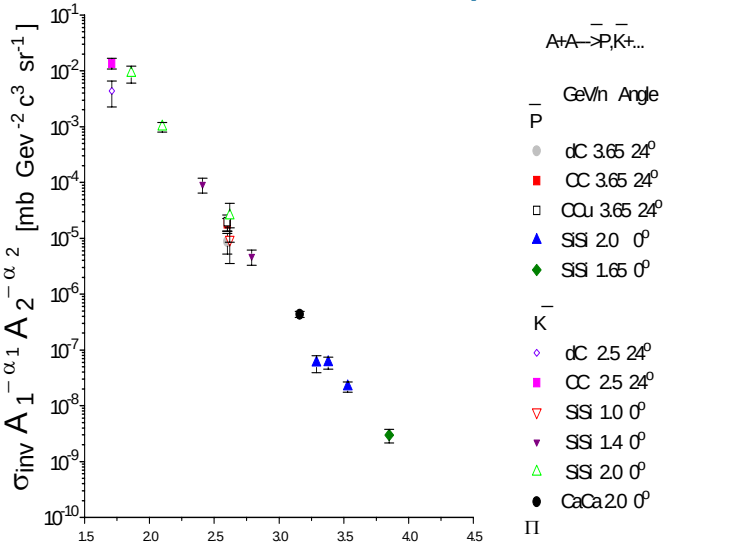

Twice cumulative deep subthreshold processes with heavy nuclei.

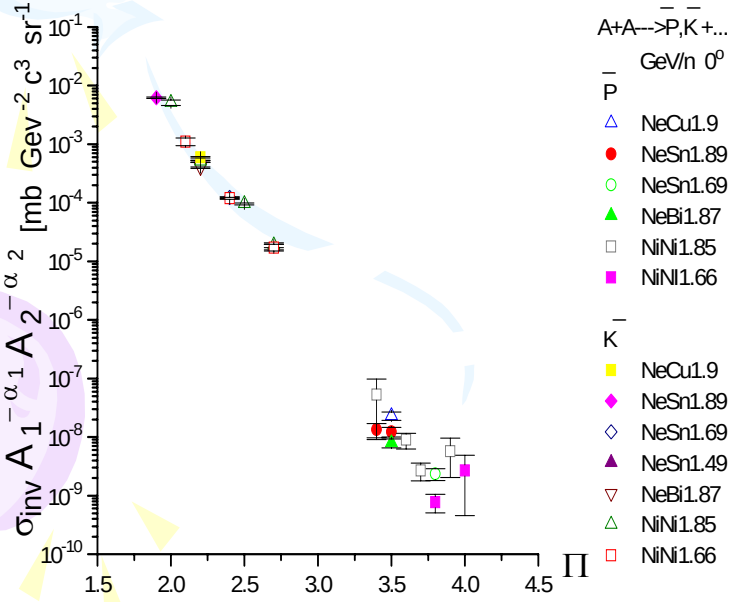

Antimatter production.

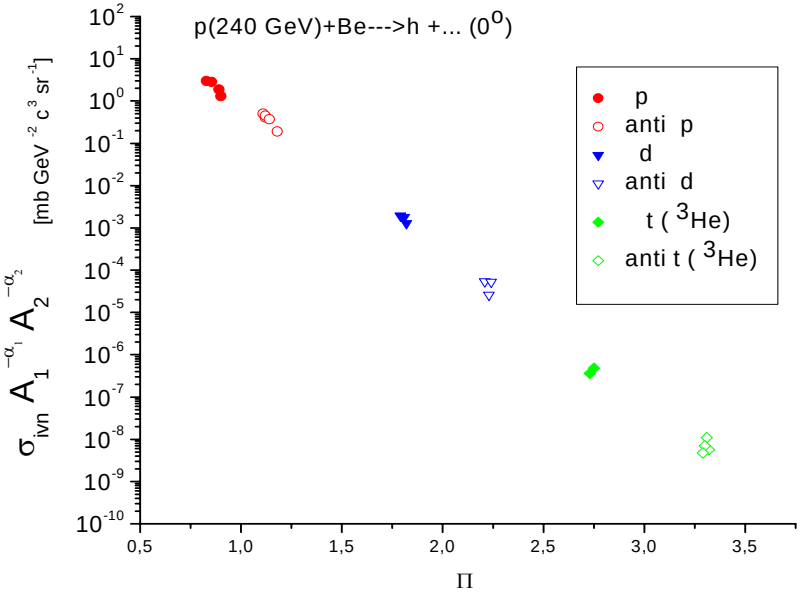

Energy Dependence of Charged Pions Produced at 180° in 0.8–4.89-GeV Proton-Nucleus Collisions

L. S. Schroeder, S. A. Chessin, J. V. Geaga, J. Y. Grossiord,[a]
J. W. Harris, D. L. Hendrie, R. Treuhaft, and K. Van Bibber
Lawrence Berkeley Laboratory, University of California, Berkeley, California 94720
(Received 25 September 1979)

High-energy charged pions produced at 180° in 0.8–4.89-GeV proton-nucleus collisions have been studied. Both the slopes of the energy spectra and the π^-/π^+ ratios increase rapidly with primary energy up to ~3–4 GeV, where limiting values appear to be reached. The dependence on target mass also changes over this energy range. Unlike forward pion-production results, backward pions at these energies do not obey the scaling law suggested by Schmidt and Blankenbecler.

We report on a systematic study of the energy dependence of charged pions produced at 180° in the collisions of 0.8–4.89-GeV protons with nuclei. A principal reason for studying production of energetic pions from nuclei in the backward direction is that in free nucleon-nucleon (N-N) collisions such production is kinematically restricted. Observation of pions beyond this kinematic limit may then be evidence for exotic production mechanisms such as production from clusters.[1-5] Early experiments by Baldin *et al.*[6] using 5.14- and 7.52-GeV protons observed

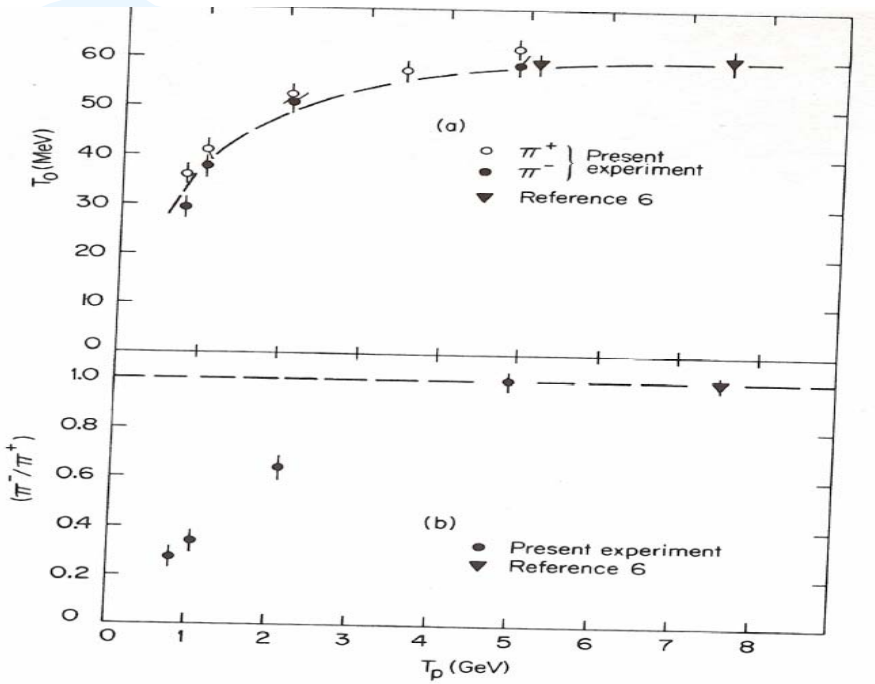

FIG. 1. Energy dependence of (a) T_0 parameter for pions, and (b) the π^-/π^+ ratio at 180° obtained by integrating each spectra up to 100 MeV for p-Cu collisions from 0.8 to 4.89 GeV. The dashed curve in both cases refers to the predictions of the "effective-target" model (Refs. 3 and 4).

tering mechanism to one where nucleon clusters play an ever increasing role. To isolate the production mechanism further, experiments are required which will measure additional observables such as associated multiplicities and two-particle correlations. However, it is clear that by measuring the production of pions in kinematic regions beyond those available in free N-N collisions, such as at 180° and high energies, one is probing the short-range behavior of nucleons in nuclei. This behavior might manifest itself as large Fermi momenta or nucleon clusters.

Subthreshold flucton-flucton production

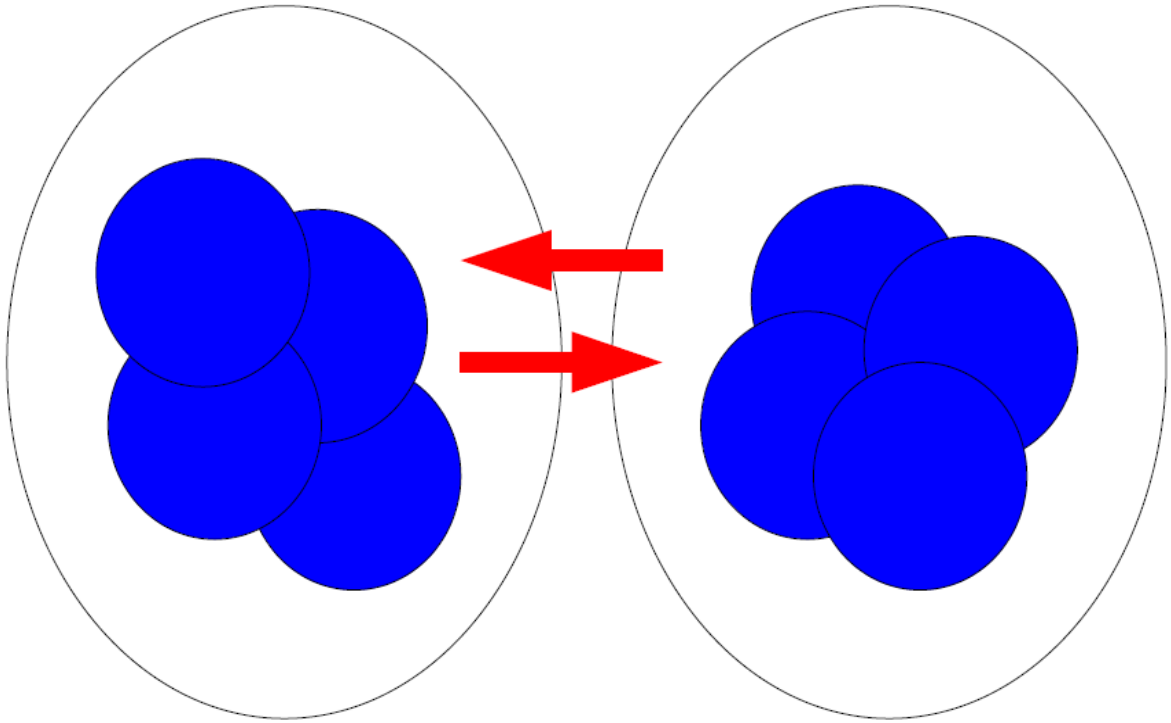

$$\sigma_h \sim P^2{}_K \cdot G^2{}_{h/K}(K)$$

Inverse slope for subthreshold production must be the less then $T_0/2$
(near the phase space border).

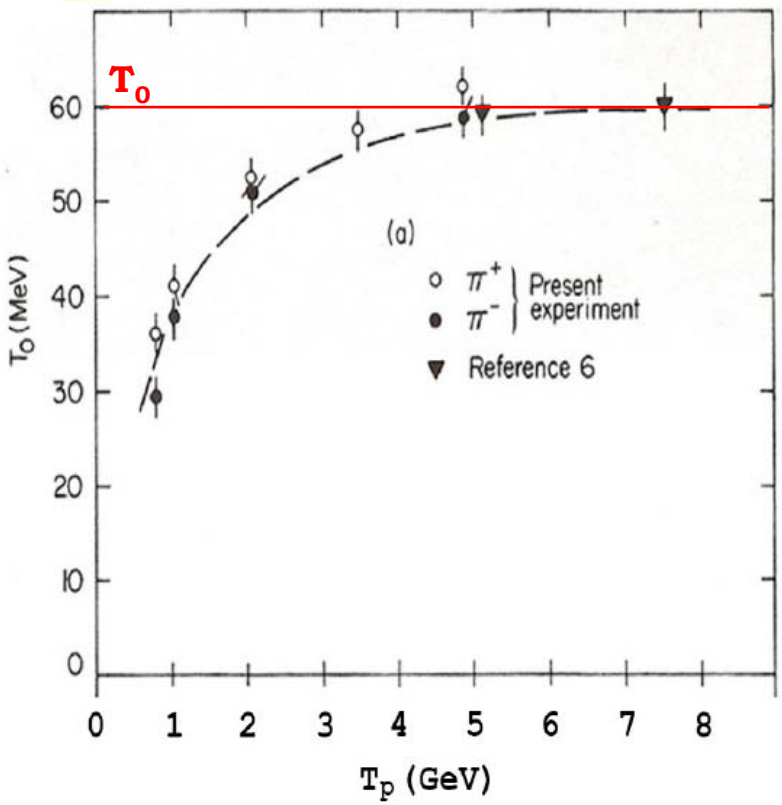

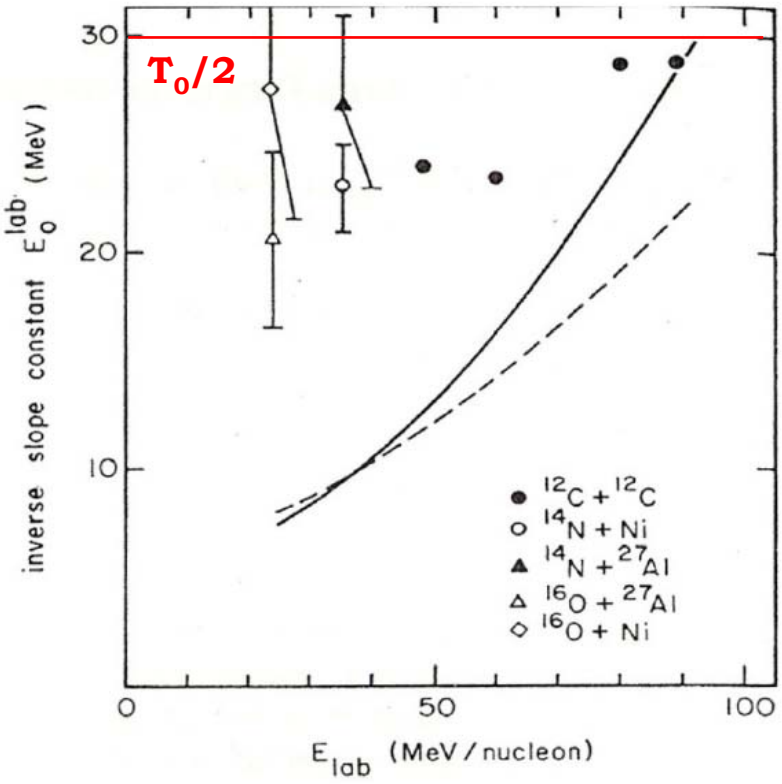

$$P_{cum} \sim \exp\left(-T/T_0\right) \quad \Rightarrow \quad P_{subthresh} \sim \exp\left(-T/T_0\right) \cdot \exp\left(-T/T_0\right) \sim \exp\left(-T/(T_0/2)\right)$$

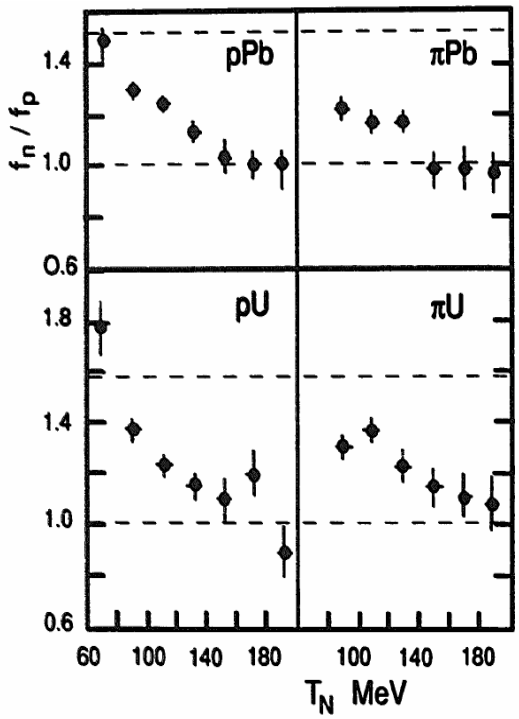

Figure 3 : Ratio of neutron to proton yields for various nuclei and various probes, as a function of the energy of the secondary hadron

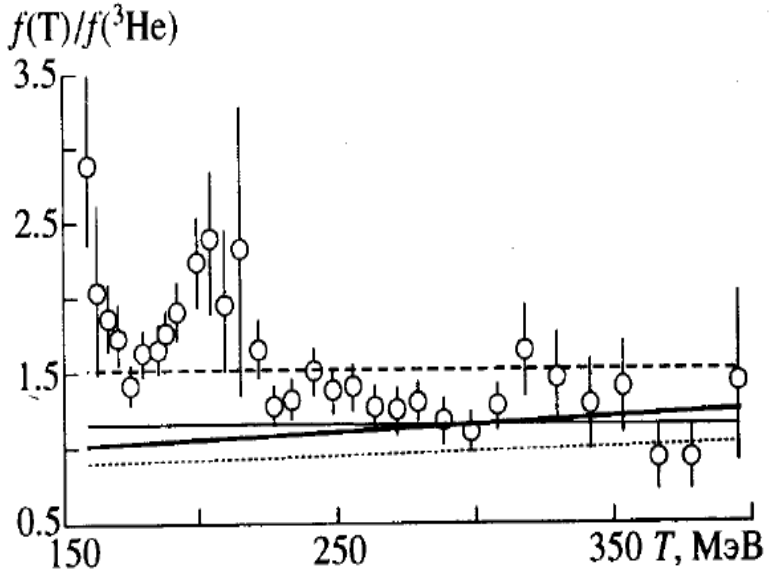

Рис. 9. Зависимость отношения $T/^3He$ от кинетической энергии вторичных частиц. Угол $\theta = 90°$, ядро – Pb. Обозначения кривых аналогичны рис. 1.

ЯДЕРНАЯ ФИЗИКА, 2002, том 65, № 11, с. 2042–2051

ПУТИ ИССЛЕДОВАНИЯ ЯДЕРНОГО ВЕЩЕСТВА В УСЛОВИЯХ, ХАРАКТЕРНЫХ ДЛЯ ЕГО ПЕРЕХОДА В КВАРК-ГЛЮОННУЮ ПЛАЗМУ

© 2002 г. Г. А. Лексин

Институт теоретической и экспериментальной физики, Москва, Россия

Поступила в редакцию 07.02.2002 г.

Кратко представлены свойства глубоконеупругих ядерных реакций, происходящих на плотных флуктуациях ядерной материи (флуктонах). Обсуждаются свойства флуктонов, которыми могут быть многокварковые "мешки" или "капельки" кварк-глюонной плазмы: характерные параметры ядерного вещества во флуктоне — "температура" и плотность порядка критических для фазового перехода. Их значения могут быть достигнуты или превзойдены, если выделить события флуктон-флуктонных столкновений. Обсуждается способ выделения.

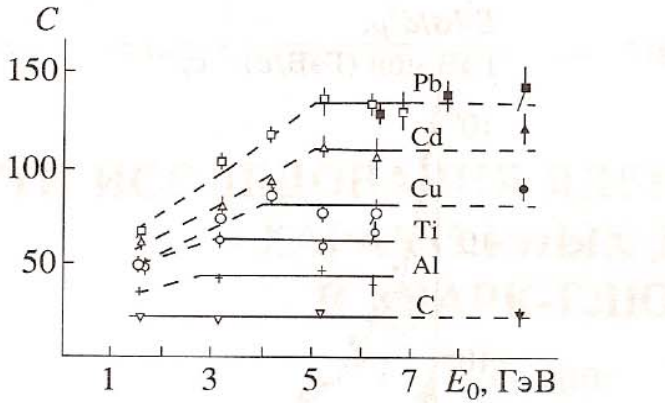

Рис. 3. Зависимость коэффициента $C(T_0 = 125$ МэВ) в параметризации инвариантной функции $f = C \times \times \exp(-T/T_0)$ в реакции pA(C, Al, Ti, Cu, Cd, Pb) $\rightarrow$ $\rightarrow pX$ для угла вылета протонов 120° в л.с. от энергии налетающих протонов. Черные точки справа относятся к начальной энергии 400 ГэВ.

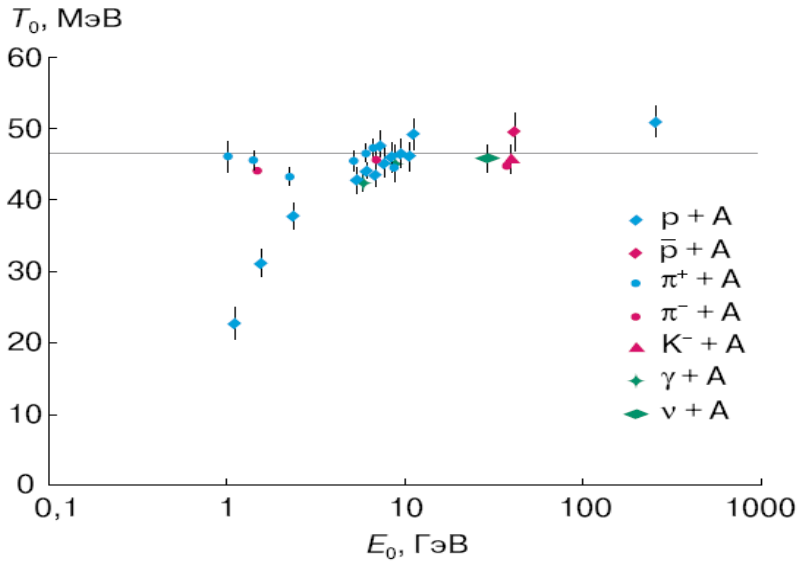

Рис. 3. Зависимость наклонов инвариантных функций кумулятивных протонов, вылетающих под углом 120°, от энергии различных налетающих частиц.

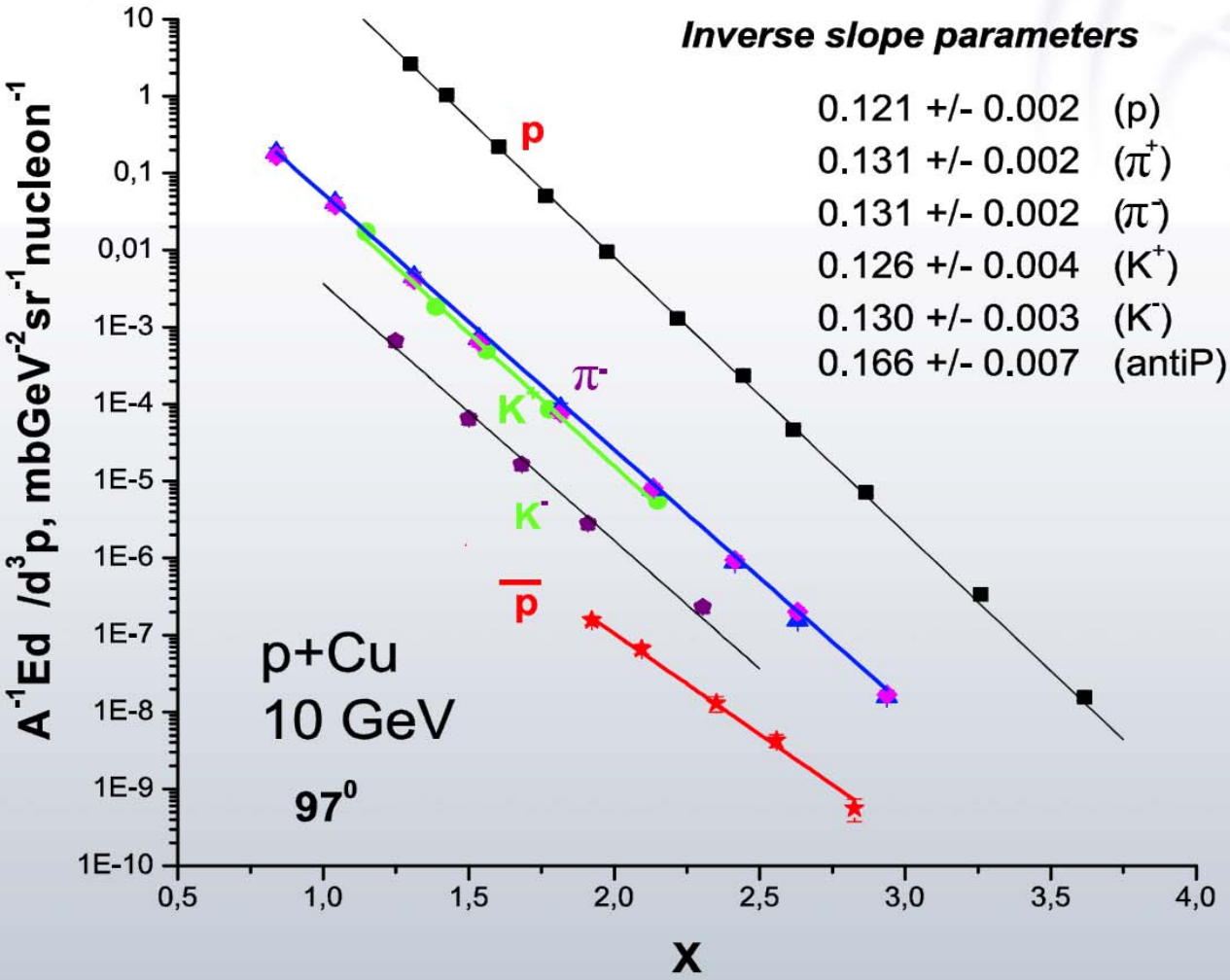

FAS @ ITEP
(Boyarinov et.al
Yad.Fiz 57
(1994) 1452)

X – minimal target mass [m_N] needed to produce particle

Flucton hypothesis

$$\bar{p} + A \rightarrow \pi, \kappa, J/\Psi, p, n, \ldots + X$$

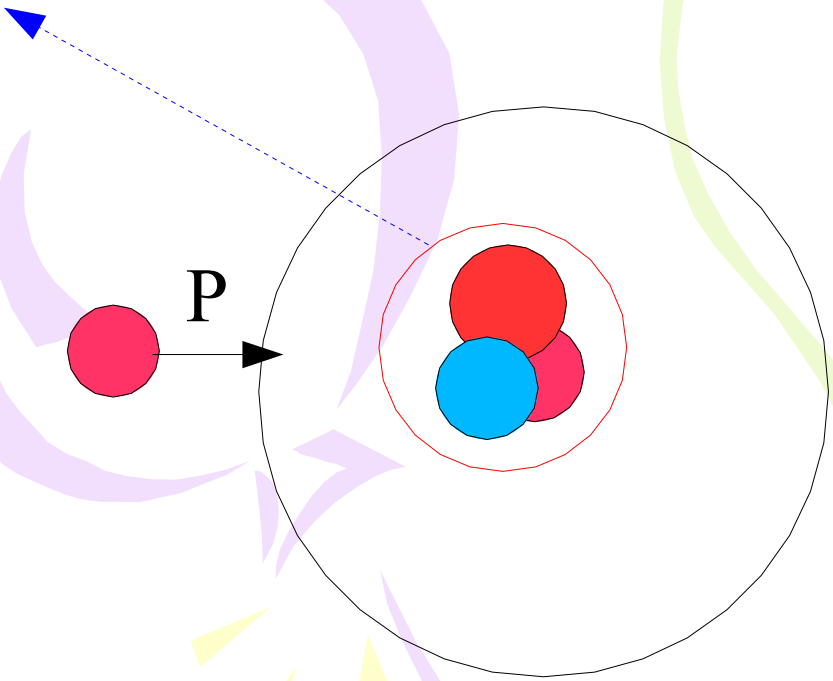

$$\sigma_h \sim P_K \cdot G_{h/K}(K)$$

Fermi motion or Short Range Correlation (SRC) mechanism

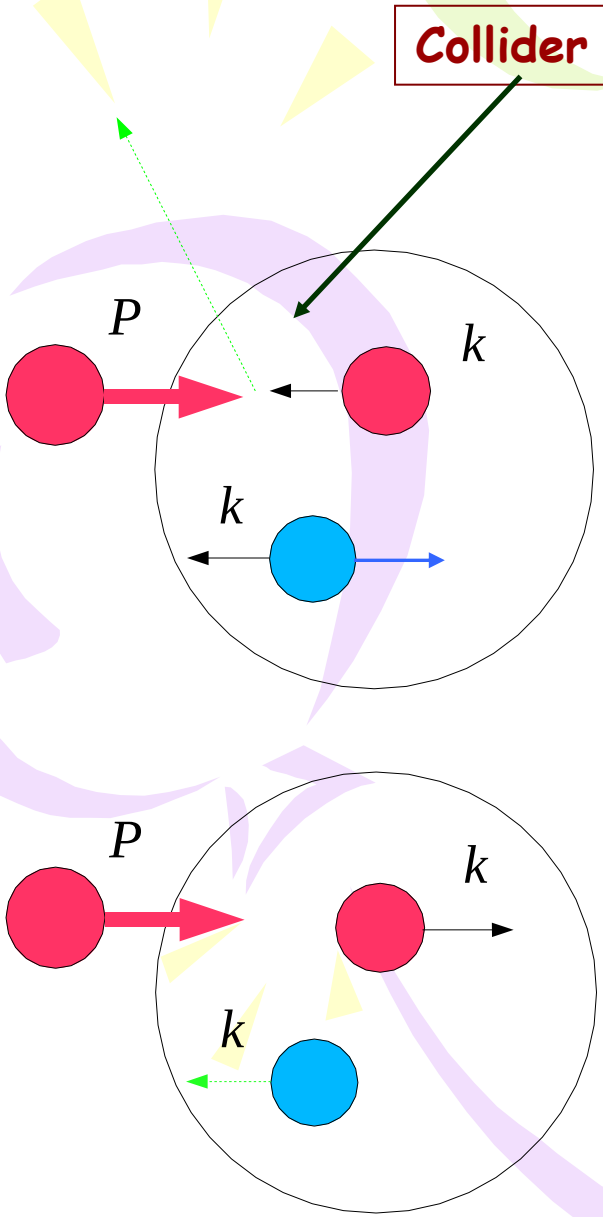

$$\bar{p} + A \to \pi, K, J/\Psi, \ldots + X$$

$$\sigma_\pi \sim n(\vec{k}) \cdot \sigma(\bar{p}N \to \pi, K + \bar{p} + X)$$

$$\bar{p} + A \to n, p, \ldots + \bar{p} + X$$

$$\sigma_N \sim n(\vec{k}) \cdot \sigma_0$$

Volume 67B, number 1 PHYSICS LETTERS 14 March 1977

ТЕОРИЯ

LARGE MOMENTUM PION PRODUCTION IN PROTON NUCLEUS COLLISIONS AND THE IDEA OF "FLUCTUONS" IN NUCLEI

V.V. BUROV
The Moscow State University, Moscow, USSR

and

V.K. LUKYANOV and A.I. TITOV
Joint Institute for Nuclear Research, Dubna, USSR

Received 27 January 1977

It is shown that in proton-nucleus collisions, the production of pions with large momenta can be explained by the assumption of the existence of nuclear density fluctuations ("fluctuons") at short distances of the nucleon core radius order, with the mass of several nucleons.

The purpose of this note is to realize the idea [4] that the cumulative effect is connected largely with a suggestion on the existence in nuclei of the so-called fluctuons. Earlier fluctuons were proposed [7] in order to understand the nature of the "deuteron peak" in the pA-scattering cross section at large momentum transfers [8] and also to interpret the pd-scattering cross section [9]. Compressional fluctuations of mass $M_k = km_p$ of nucleons in the small volume $V_\xi = \frac{4}{3}\pi r_\xi^3$ where r_ξ is the fluctuon radius were assumed.

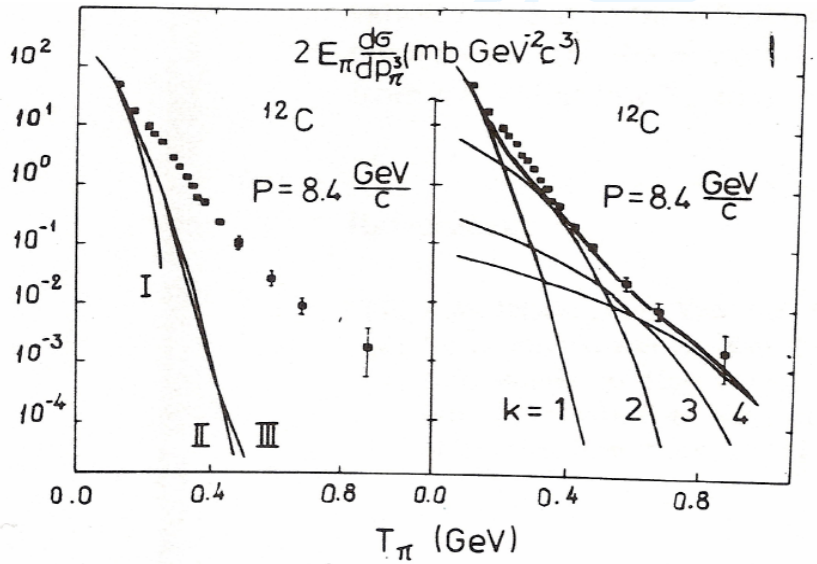

Fig. 1. (a) Calculations of the invariant pion production cross section for ^{12}C: I – for the free proton target; II – with fermi motion; III – the relativization effect. (b) The contributions of separate fluctuons with mass $M_k = km_p$ where k is the order of cumulativity.

12. ВЕРОЯТНОСТЬ СУЩЕСТВОВАНИЯ ФЛУКТОНОВ В ЯДРАХ

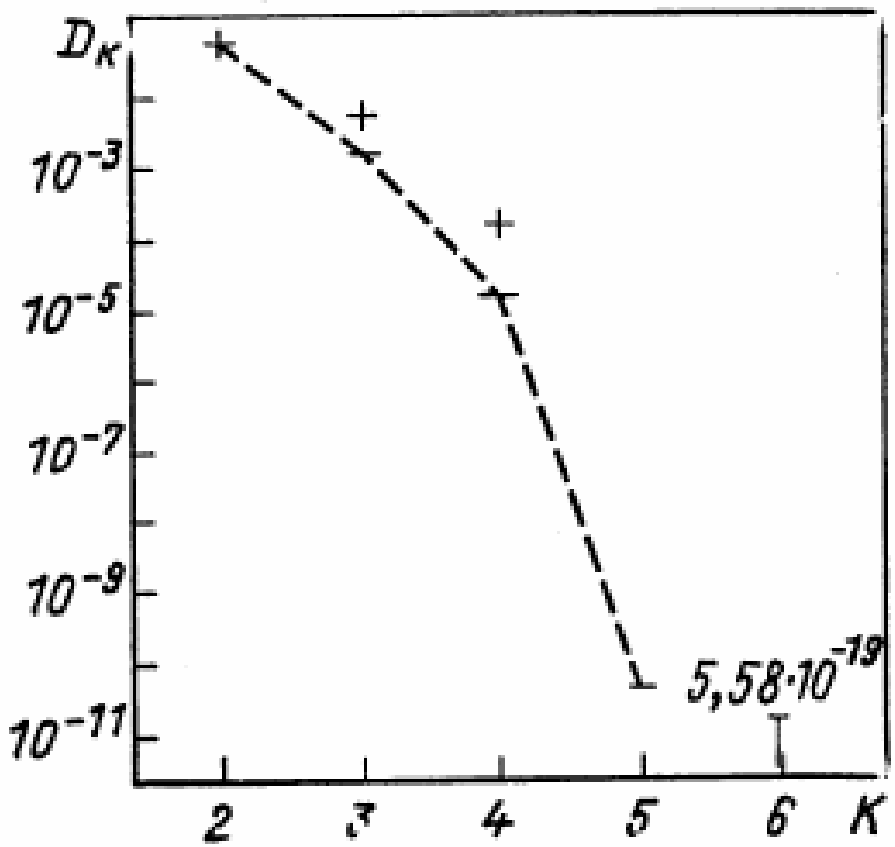

Рис. 19. Вероятность существования флуктонов с k нуклонами в ядрах

Forward K^+ Production in Subthreshold pA Collisions at 1.0 GeV

V. Koptev,[1] M. Büscher,[2] H. Junghans,[2] M. Nekipelov,[1,2] K. Sistemich,[2] H. Ströher,[2] V. Abaev,[1] H.-H. Adam,[3] R. Baldauf,[4] S. Barsov,[1] U. Bechstedt,[2] N. Bongers,[2] G. Borchert,[2] W. Borgs,[2] W. Bräutigam,[2] W. Cassing,[5] V. Chernyshev,[6] B. Chiladze,[7] M. Debowski,[8] J. Dietrich,[2] M. Drochner,[4] S. Dymov,[9] J. Ernst,[10] W. Erven,[4] R. Esser,[11,*] P. Fedorets,[6] A. Franzen,[2] D. Gotta,[2] T. Grande,[2] D. Grzonka,[2] G. Hansen,[12] M. Hartmann,[2] V. Hejny,[2] L. v. Horn,[2] L. Jarczyk,[13] A. Kacharava,[9] B. Kamys,[13] A. Khoukaz,[3] T. Kirchner,[8] S. Kistryn,[13] F. Klehr,[12] H. R. Koch,[2] V. Komarov,[9] S. Kopyto,[2] R. Krause,[2] P. Kravtsov,[1] V. Kruglov,[9] P. Kulessa,[2,15] A. Kulikov,[9,14] V. Kurbatov,[9] N. Lang,[3] N. Langenhagen,[8] I. Lehmann,[2] A. Lepges,[2] J. Ley,[11] B. Lorentz,[2] G. Macharashvili,[7,9] R. Maier,[2] S. Martin,[2] S. Merzliakov,[9] K. Meyer,[2] S. Mikirtychiants,[1] H. Müller,[8] P. Munhofen,[2] A. Mussgiller,[2] V. Nelyubin,[1] M. Nioradze,[7] H. Ohm,[2] A. Petrus,[9] D. Prasuhn,[2] B. Prietzschk,[8] H. J. Probst,[2] D. Protic,[2] K. Pysz,[15] F. Rathmann,[2] B. Rimarzig,[8] Z. Rudy,[13] R. Santo,[3] H. Paetz gen. Schieck,[11] R. Schleichert,[2] A. Schneider,[2] Chr. Schneider,[8] H. Schneider,[2] G. Schug,[2] O. W. B. Schult,[2] H. Seyfarth,[2] A. Sibirtsev,[2] J. Smyrski,[13] H. Stechemesser,[12] E. Steffens,[16] H. J. Stein,[2] A. Strzalkowski,[13] K.-H. Watzlawik,[2] C. Wilkin,[17] P. Wüstner,[4] S. Yashenko,[9] B. Zalikhanov,[9] N. Zhuravlev,[9] P. Zolnierczuk,[13] K. Zwoll,[4] and I. Zychor[18]

K^+-meson production in pA (A = C, Cu, Au) collisions has been studied using the ANKE spectrometer at an internal target position of the COSY-Jülich accelerator. The complete momentum spectrum of kaons emitted at forward angles, $\vartheta \leq 12°$, has been measured for a beam energy of $T_p = 1.0$ GeV, far below the free NN threshold of 1.58 GeV. The spectrum does not follow a thermal distribution at low kaon momenta and the larger momenta reflect a high degree of collectivity in the target nucleus.

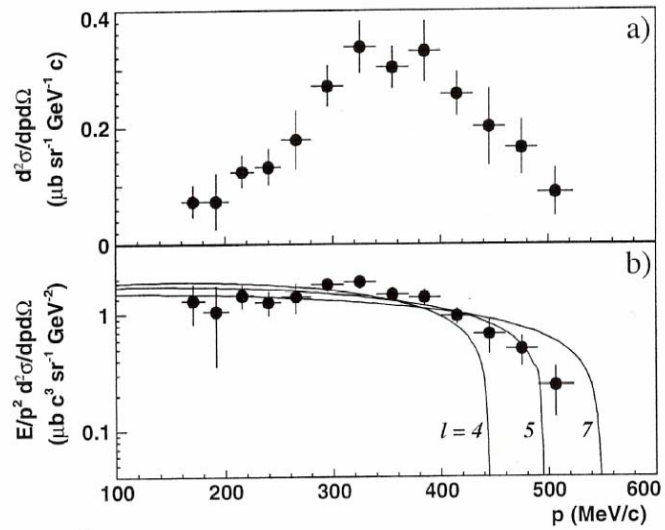

FIG. 2. (a) Double differential K^+-production cross section for the $p(1.0\ \text{GeV})^{12}\text{C} \rightarrow K^+(\vartheta \leq 12°)X$ reaction as a function of the K^+ momentum. (b) Same data plotted as invariant cross section. The error bars are purely statistical. The overall normalization uncertainty is estimated to be 10%. The solid lines describe the behavior of the invariant cross section within a phase-space approximation [Eq. (2)].

K.Rith From Nuclei to Nucleons (Summary)
Nuclear Physics A532 (1991) 3c-14c

2.6. Region 5

In the region $x > 1$ the struck quark is 'superfast', its momentum is larger than the momentum allowed for a stationary nucleon. The longitudinal distances involved are $z < 0.2$ fm and therefore one is sensitive to correlations of nearby nucleons or more complicated configurations like multiquark clusters. As an example the predictions for a multiquark cluster calculation [32] are shown in figure 5.

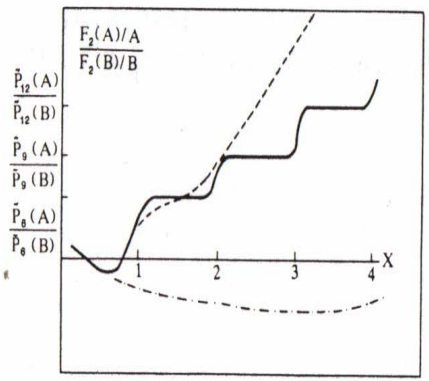

Figure 5. Theoretical predictions for nuclear structure functions at $x > 1$

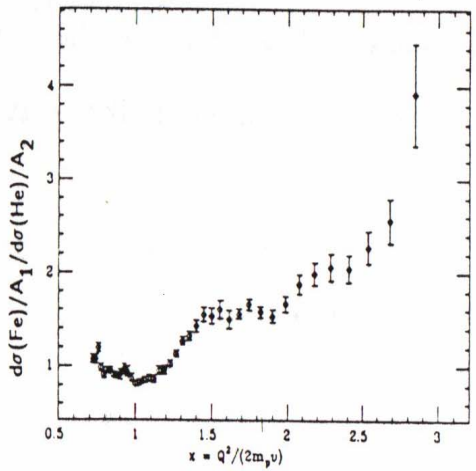

Figure 6. Preliminary results for σ^{Fe}/σ^{He} from NE-2 at SLAC

The height of the plateau in the range $1 < x < 2$ is proportional to the ratio of probabilities of finding 6-quark clusters in nuclei A and B, the range $2 < x < 3$ reflects the ratio of 9-quark cluster probabilities and so on.

Figure 6 shows preliminary results for the cross section ratio of Fe and He obtained by NE-2 at SLAC [33], which took data for a series of nuclei with beam energies between 4 and 14 GeV. One could speculate that the plateau for $1.5 < x < 2$ is an indication for the step function expected in the multiquark cluster model. Note, however, that the data are still substantially affected by quasielastic scattering as the ratio is smaller than one near $x = 1$.

32 J. Vary, Proceedings of the 7th Int. Conf. on High Energy Physics problems, Dubna 1984,147.

INSTITUTE OF PHYSICS PUBLISHING JOURNAL OF PHYSICS G: NUCLEAR AND PARTICLE PHYSICS

J. Phys. G: Nucl. Part. Phys. **29** (2003) R1–R45 PII: S0954-3899(03)54926-X

JLAB data

TOPICAL REVIEW

Hadrons in the nuclear medium

M M Sargsian[1], J Arrington[2], W Bertozzi[3], W Boeglin[1], C E Carlson[4], D B Day[5], L L Frankfurt[6], K Egiyan[7], R Ent[8], S Gilad[3], K Griffioen[4], D W Higinbotham[8], S Kuhn[9], W Melnitchouk[8], G A Miller[10], E Piasetzky[6], S Stepanyan[8,9], M I Strikman[11] and L B Weinstein[9]

Abstract

Quantum chromodynamics (QCD), the microscopic theory of strong interactions, has not yet been applied to the calculation of nuclear wavefunctions. However, it certainly provokes a number of specific questions and suggests the existence of novel phenomena in nuclear physics which are not part of the traditional framework of the meson–nucleon description of nuclei. Many of these phenomena are related to high nuclear densities and the role of colour in nucleonic interactions. Quantum fluctuations in the spatial separation between nucleons may lead to local high-density configurations of cold nuclear matter in nuclei, up to four times larger than typical nuclear densities. We argue here that experiments utilizing the higher energies available upon completion of the Jefferson Laboratory energy upgrade will be able to probe the quark–gluon structure of such high-density configurations and therefore elucidate the fundamental nature of nuclear matter. We review three key experimental programmes: quasi-elastic electro-disintegration of light nuclei, deep inelastic scattering from nuclei at $x > 1$ and the measurement of tagged structure functions. These interrelated programmes are all aimed at the exploration of the quark structure of high-density nuclear configurations.

(a) Experiments performed at electron machines with low incident electron energies, $E_{\rm inc} \leqslant 1$ GeV, in which the typical energy and momentum transfers, ν and $\vec{q}$, were comparable to the nuclear scale

$$\nu \leqslant 100\ \text{MeV}, \qquad |\vec{q}| \leqslant 2k_F, \tag{1}$$

where $k_F \approx 250$ MeV/c is the characteristic Fermi momentum of nuclei. These reactions were inclusive (e, e') and semi-inclusive $(e, e'N)$ and covered mainly the quasi-elastic and the low lying resonance regions (the Δ isobars), corresponding to relatively large values of Bjorken-x ($x = Q^2/2m_p\nu$, where $Q^2 = q^2 - \nu^2$).

(b) Deep inelastic scattering (DIS) experiments which probed nuclei at $x < 1$ and large Q^2 scales, greater than about 4 GeV^2, which resolved the parton constituents of the nucleus.

The first class of experiments is unable to resolve the short-range structure of nuclei, and the second, while having good resolution, typically involved inclusive measurements which averaged out the fine details and were limited by low luminosities and other factors.

It is interesting to note that there is a clear gap between the kinematic regions of these two classes of experiments. This corresponds exactly to the optimal range for the study of the nucleonic degrees of freedom in nuclei, $1.5 \leqslant Q^2 \leqslant 4$ GeV^2, for which short-range correlations (SRCs) between nucleons can be resolved, and the quark degrees of freedom are only a small correction. Work at Jefferson Lab has started to fill this gap in a series of quasi-elastic $A(e, e')$, $A(e, e'N)$ and $A(e, e'N_1N_2)$ experiments. Previously, this range was just touched by inclusive experiments at SLAC [2–5] which also provided the first measurement of $A = 2, 3, 4$ form factors at large Q^2. A number of these high-energy experiments probe the light-cone projection of the nuclear wavefunction and in particular the light-cone nuclear density matrix, $\rho_A^N(\alpha, p_\perp)$, in the kinematics where the light-cone momentum fraction $\alpha \geqslant 1$ ($A \geqslant \alpha \geqslant 0$) so that short-range correlations between nucleons play an important role.

Shimanskiy S.S.

JLAB data

A.Stavinskiy, ITEP seminar, 11.4.2007

2 nucleon correlations

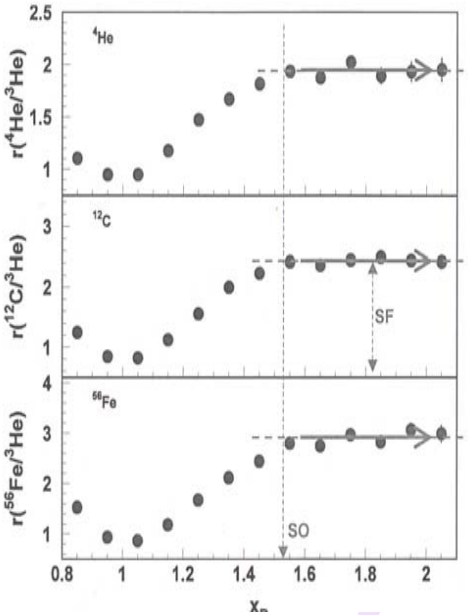

relative to ^{3}He

$\frac{a_{2N}(^4He)}{a_{2N}(^3He)}$ =1.93±0.02±0.14

= 0.080+0.016 From ^{2}H and ^{3}He wave functions

$\frac{a_{2N}(^{12}C)}{a_{2N}(^3He)}$ =2.41±0.02±0.17

$\frac{a_{2N}(^{56}Fe)}{a_{2N}(^3He)}$ =2.83±0.03±0.18

Absolute fraction

$a_{2N}(^4He)$ = 0.154±0.002±0.033

$a_{2N}(^{12}C)$ = 0.193±0.002±0.041

$a_{2N}(^{56}Fe)$ = 0.23±0.002±0.047

3 nucleon correlations

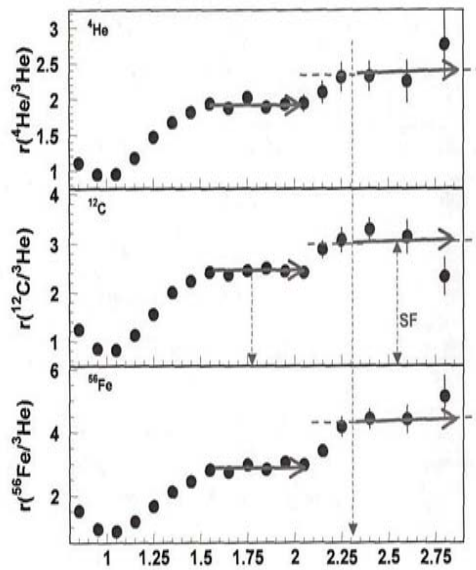

relative to ^{3}He

$\frac{a_{3N}(^4He)}{a_{3N}(^3He)}$ = 2.33±0.12±0.19

= 0.0018±0.0006 (M. Sargsyan's calculations)

$\frac{a_{3N}(^{12}C)}{a_{3N}(^3He)}$ =3.05±0.14±0.22

$\frac{a_{3N}(^{56}Fe)}{a_{3N}(^3He)}$ = 4.38±0.18±0.33

Absolute fraction

$a_{3N}(^4He)$= 0.42±0.02±0.14

$a_{3N}(^{12}C)$= 0.55±0.03±0.18

$a_{3N}(^{56}Fe)$= 0.79±0.03±0.25

Shimanskiy S.S.

JLAB data

Having these data, we know almost full (≈99%) nucleonic picture of nuclei with A ≤ 56

Fractions / Nucleus	Single particle (%)	2N SRC (%)	3N SRC (%)
^{56}Fe	**76** ± 0.2 ± 4.7	**23.0** ± 0.2 ± 4.7	**0.79** ± 0.03 ± 0.25
^{12}C	**80** ± 02 ± 4.1	**19.3** ± 0.2 ± 4.1	**0.55** ± 0.03 ±0.18
^{4}He	**86** ± 0.2 ± 3.3	**15.4** ± 0.2 ± 3.3	**0.42** ± 0.02 ± 0.14
^{3}He	**92** ± 1.6	**8.0** ± 1.6	**0.18** ± 0.06
^{2}H	**96** ± 0.8	**4.0** ± 0.8	-----

Using the published data on (p,2p+n) [PRL,90 (2003) 042301] estimate the isotopic composition of 2N SRC in ^{12}C

$a_{2N}(^{12}C) \approx 20 \pm 0.2 \pm 4.1$ % →

$a_{pp}(^{12}C) \approx 4 \pm 2$ %

$a_{pn}(^{12}C) \approx 12 \pm 4$ %

$a_{nn}(^{12}C) \approx 4 \pm 2$ %

Search for Sub-threshold Photoproduction of J/ψ Mesons

P. Bosted,[1] J. Dunne,[2] C. A. Lee,[3] P. Junnarkar,[2] M. Strikman,[4] J. Arrington,[5]
R. Asaturyan,[6] F. Benmokhtar,[7] M.E. Christy,[8] E. Chudakov,[1] B. Clasie,[9]
S. H. Connell,[10] M. M. Dalton,[3] A. Daniel,[11] D. Day,[12] D. Dutta,[2] R. Ent,[1]
N. Fomin,[12] D. Gaskell,[1] T. Horn,[7,1] N. Kalantarians,[11] C.E. Keppel,[8]
D.G. Meekins,[1] H. Mkrtchyan,[6] T. Navasardyan,[6] J. Roche,[1] V. M. Rodriguez,[11,13]
D. Kiselev (nee Rohe),[14,15] J. Seely,[9] K. Slifer,[12,16] S. Tajima,[12] G. Testa,[14]
Roman Trojer,[14] F.R. Wesselmann,[17] S.A. Wood,[1] and X.C. Zheng[12]

Abstract

A search was made for sub-threshold J/ψ production from a carbon target using a mixed real and quasi-real Bremsstrahlung photon beam with an endpoint energy of 5.76 GeV. No events were observed, which is consistent with predictions assuming quasi-free production. The results place limits on exotic mechanisms that strongly enhance quasi-free production.

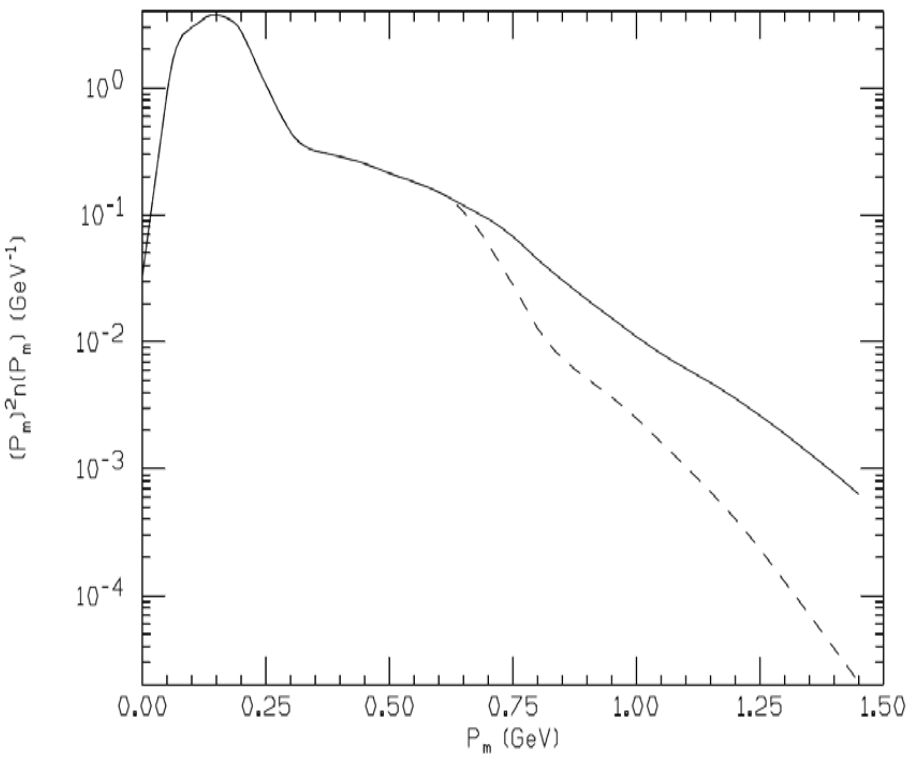

FIG. 6: The E_m-integrated probability of finding a nucleon with missing momentum P_m as a function of P_m. The solid (dashed) lines are "high" and "low" eyeball extrapolations above 0.6 GeV of the spectral function of Ref. [12].

We used three different free nucleon cross sections (as motivated by the discussion in the introduction):

$$\text{I.}\quad d\sigma/dt = ae^{bt} \tag{4}$$

$$\text{II.}\quad d\sigma/dt = a/(1-bt)^4 \tag{5}$$

$$\text{III.}\quad d\sigma/dt = a(1-x)^2/(1-bt)^4, \tag{6}$$

where a and b are free parameters, and we used $x = ((m+M_J)^2 - m^2)/(s-m^2)$ For each model, we varied the t-slope parameter b within a reasonable range and, for each value of b, determined a such that the total cross section would agree with the Cornell measurement [13] of 0.7 nb at $k = 11$ GeV. The predicted counts are shown in Fig. 7 as a function of b for each

INSTITUTE OF PHYSICS PUBLISHING JOURNAL OF PHYSICS G: NUCLEAR AND PARTICLE PHYSICS

J. Phys. G: Nucl. Part. Phys. **30** (2004) 921–936 PII: S0954-3899(04)73271-5

Subthreshold antiproton production in proton–carbon reactions

V I Komarov[1], H Müller[2] and A Sibirtsev[3]

Subthreshold particle production is a collective phenomenon which is far from being completely understood. Data on subthreshold particle production can be reproduced within the ROC model by considering the interaction of the projectile with few-nucleon systems in complete analogy to the interaction with a single nucleon, also with respect to high-momentum transfer processes. It is the simultaneous consideration of the data for all particle types

$CT\ (x_T = 1)$

Color(nuclear) transparency in 90^0 c.m. quasielastic $A(p,2p)$ reactions

The incident momenta varied from 5.9 to 14.4 GeV/c, corresponding to $4.8 < Q^2 < 12.7$ (GeV/c)^2.

$$T = \frac{\frac{d\sigma}{dt}(p + "p" \rightarrow p + p)}{Z\frac{d\sigma}{dt}(p + p \rightarrow p + p)}$$

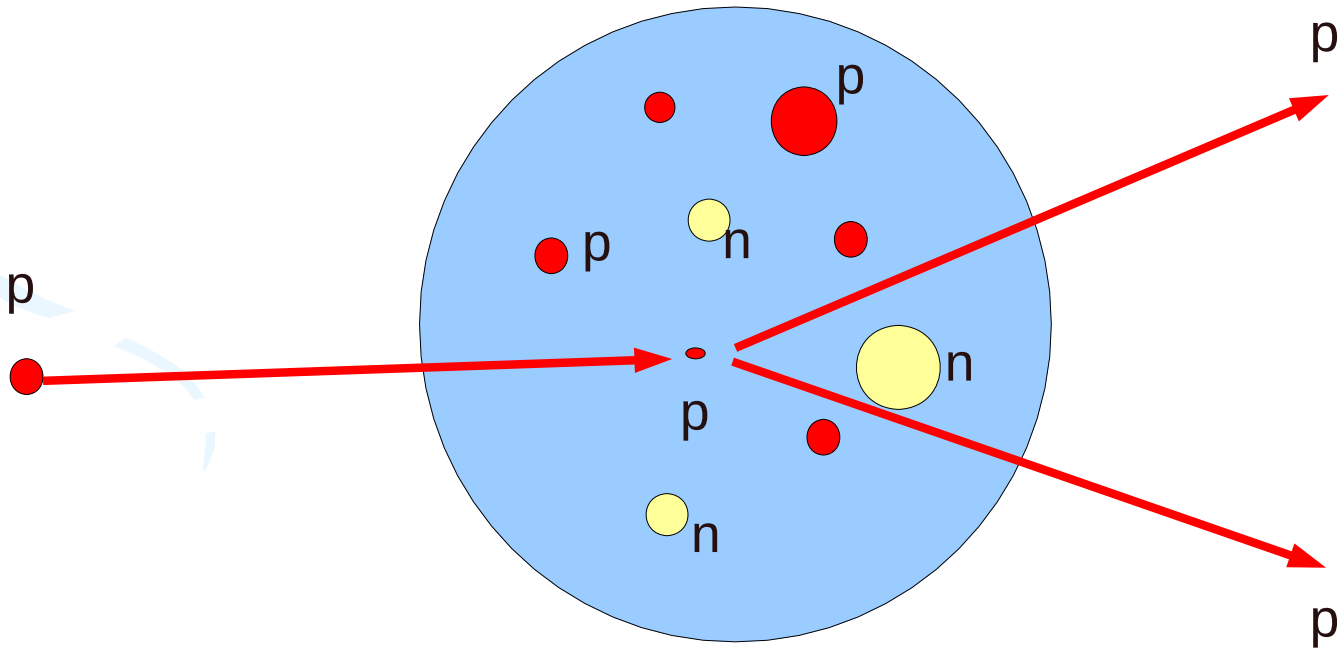

The kinematics for quasi-elastic $A(p,2p)X$ scattering.

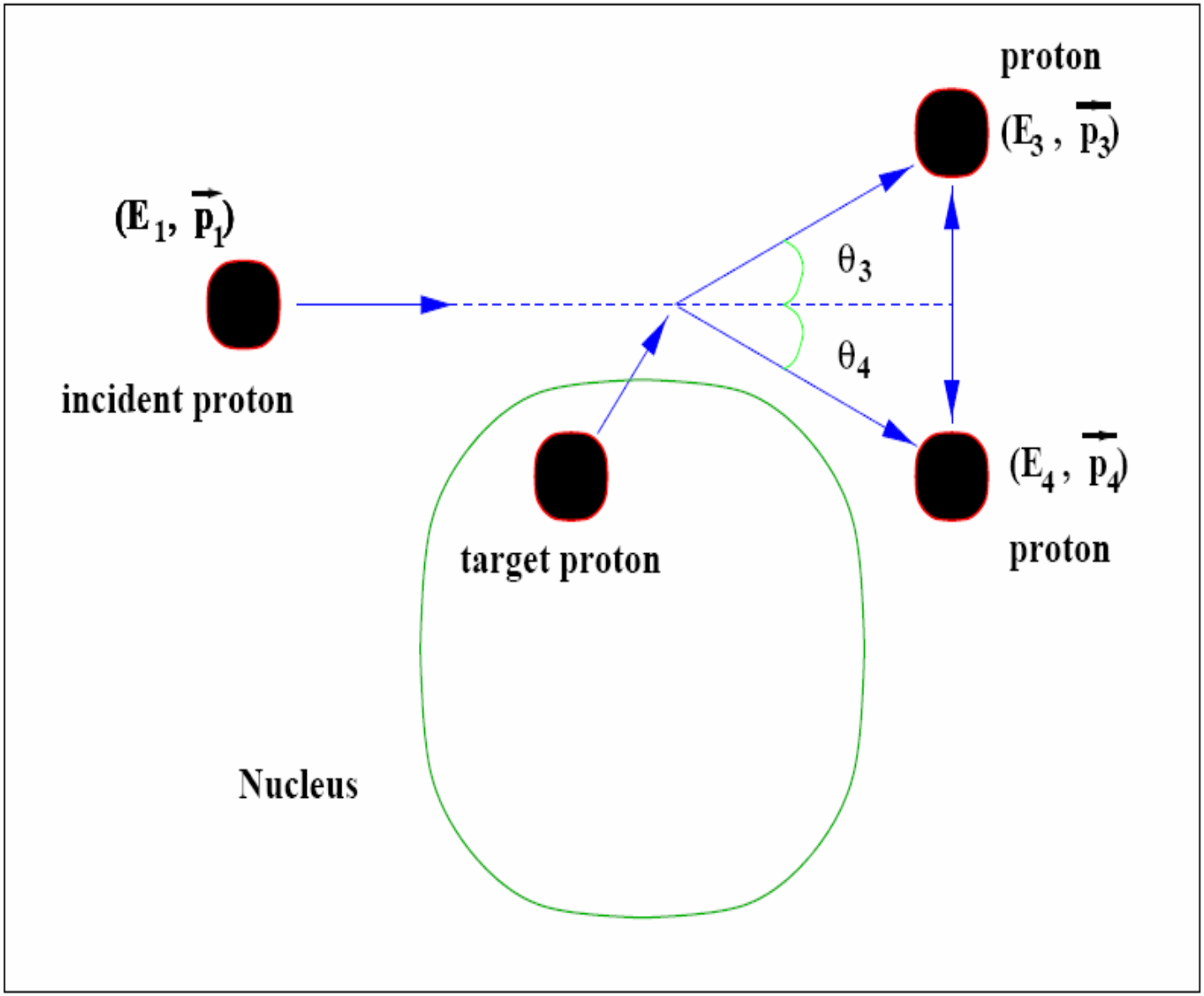

nucl-th/0608040 v2 21 Nov 2006

A relativistic framework to determine the nuclear transparency from $A(p, 2p)$ reactions

B. Van Overmeire, J. Ryckebusch

Department of Subatomic and Radiation Physics, Ghent University, Proeftuinstraat 86, B-9000 Gent, Belgium

Abstract

A relativistic framework for computing the nuclear transparency extracted $A(p, 2p)$ scattering processes is presented. The model accounts for the initia final-state interactions (IFSI) within the relativistic multiple-scattering Glaul proximation (RMSGA). For the description of color transparency, two existing els are used. The nuclear filtering mechanism is implemented as a possible ex tion for the oscillatory energy dependence of the transparency. Results are pre for the target nuclei ^{7}Li, ^{12}C, ^{27}Al, and ^{63}Cu. An approximated, computati less intensive version of the RMSGA framework is found to be sufficiently ac for the calculation of the nuclear transparency. After including the nuclear fi and color transparency mechanisms, our calculations are in acceptable agre with the data.

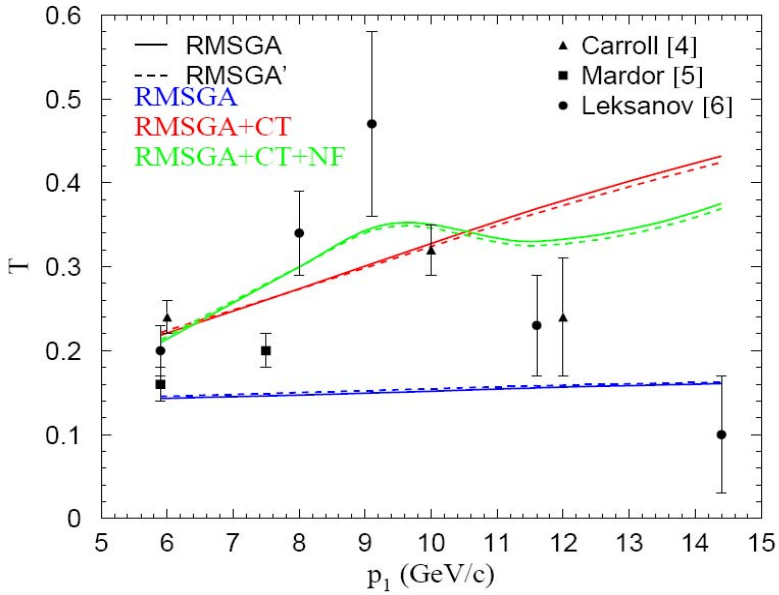

Fig. 1. The nuclear transparency for the ^{12}C$(p, 2p)$ reaction as a function the incoming lab momentum p_1. The full RMSGA (solid lines) are compared the RMSGA′ (dashed lines) results. The different curves represent the RMSG RMSGA+CT and RMSGA+CT+NF calculations. The CT effects are calculat in the FLFS model [21] with $\Delta M^2 = 0.7$ (GeV/c^2)^2 and the results including t mechanism of NF are obtained using the positive sign of $\phi(s) + \delta_1$. Data are fro Refs. [4,5,6].

Shimanskiy S.S.

Energy Dependence of Nuclear Transparency in C(p,2p) Scattering

A. Leksanov,[5] J. Alster,[1] G. Asryan,[3,2] Y. Averichev,[8] D. Barton,[3] V. Baturin,[5,4] N. Bukhtoyarova,[3,4] A. Carroll,[3] S. Heppelmann,[5] T. Kawabata,[6] Y. Makdisi,[3] A. Malki,[1] E. Minina,[5] I. Navon,[1] H. Nicholson,[7] A. Ogawa,[5] Yu. Panebratsev,[8] E. Piasetzky,[1] A. Schetkovsky,[5,4] S. Shimanskiy,[8] A. Tang,[9] J. W. Watson,[9] H. Yoshida,[6] and D. Zhalov[5]

[1]*School of Physics and Astronomy, Sackler Faculty of Exact Sciences, Tel Aviv University, Ramat Aviv 69978, Isra*
[2]*Yerevan Physics Institute, Yerevan 375036, Armenia*
[3]*Collider-Accelerator Department, Brookhaven National Laboratory, Upton, New York, 11973*
[4]*Petersburg Nuclear Physics Institute, Gatchina, St. Petersburg 188350, Russia*
[5]*Physics Department, Pennsylvania State University, University Park, Pennsylvania 16801*
[6]*Department of Physics, Kyoto University, Sakyoku, Kyoto, 606-8502, Japan*
[7]*Department of Physics, Mount Holyoke College, South Hadley, Massachusetts 01075*
[8]*J.I.N.R., Dubna, Moscow 141980, Russia*
[9]*Department of Physics, Kent State University, Kent, Ohio 44242*
(Received 20 April 2001; published 6 November 2001)

The transparency of carbon for $(p,2p)$ quasielastic events was measured at beam momenta ranging from 5.9 to 14.5 GeV/c at 90° c.m. The four-momentum transfer squared (Q^2) ranged from 4.7 to 12.7 (GeV/c)^2. We present the observed beam momentum dependence of the ratio of the carbon to hydrogen cross sections. We also apply a model for the nuclear momentum distribution of carbon to obtain the nuclear transparency. We find a sharp rise in transparency as the beam momentum is increased to 9 GeV/c and a reduction to approximately the Glauber level at higher energies.

$$T_{\mathrm{CH}} = T \int d\alpha \int d^2\vec{P}_{FT}\, n(\alpha, \vec{P}_{FT}) \frac{(\frac{d\sigma}{dt})_{pp}(s(\alpha))}{(\frac{d\sigma}{dt})_{pp}(s_0)}$$

$$\alpha \equiv A \frac{(E_F - P_{Fz})}{M_A} \simeq 1 - \frac{P_{Fz}}{m_p}$$

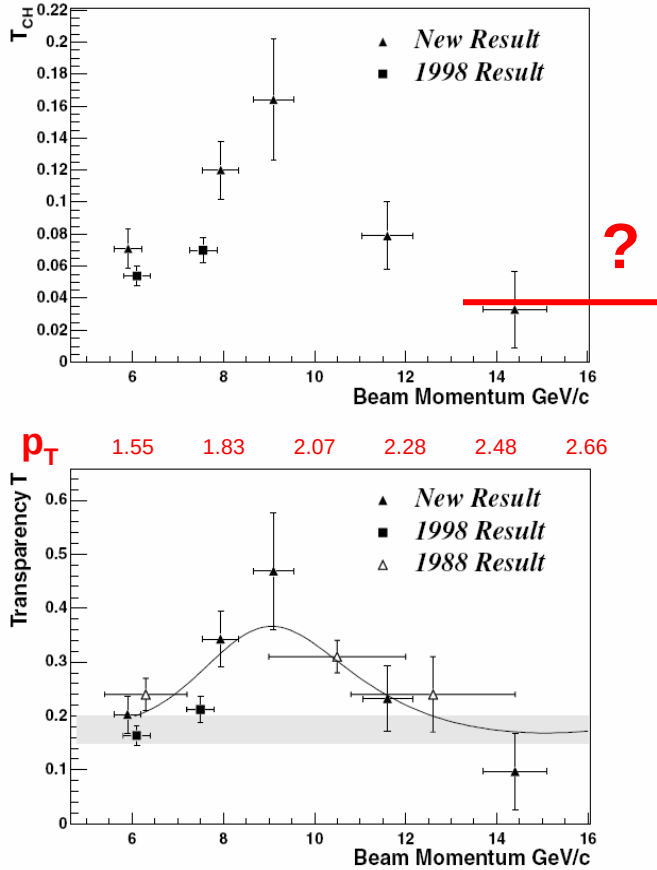

FIG. 2. Top: The transparency ratio T_{CH} as a function of the beam momentum for both the present result and two points from the 1998 publication [3]. Bottom: The transparency T versus beam momentum. The vertical errors shown here are all statistical errors, which dominate for these measurements. The horizontal errors reflect the α bin used. The shaded band represents the Glauber calculation for carbon [9]. The solid curve shows the shape R^{-1} as defined in the text. The 1998 data cover the c.m. angular region from 86°–90°. For the new data, a similar angular region is covered as is discussed in the text. The 1988 data cover 81°–90° c.m.

Shimanskiy S.S.

High p_T suppression in AA-collisions

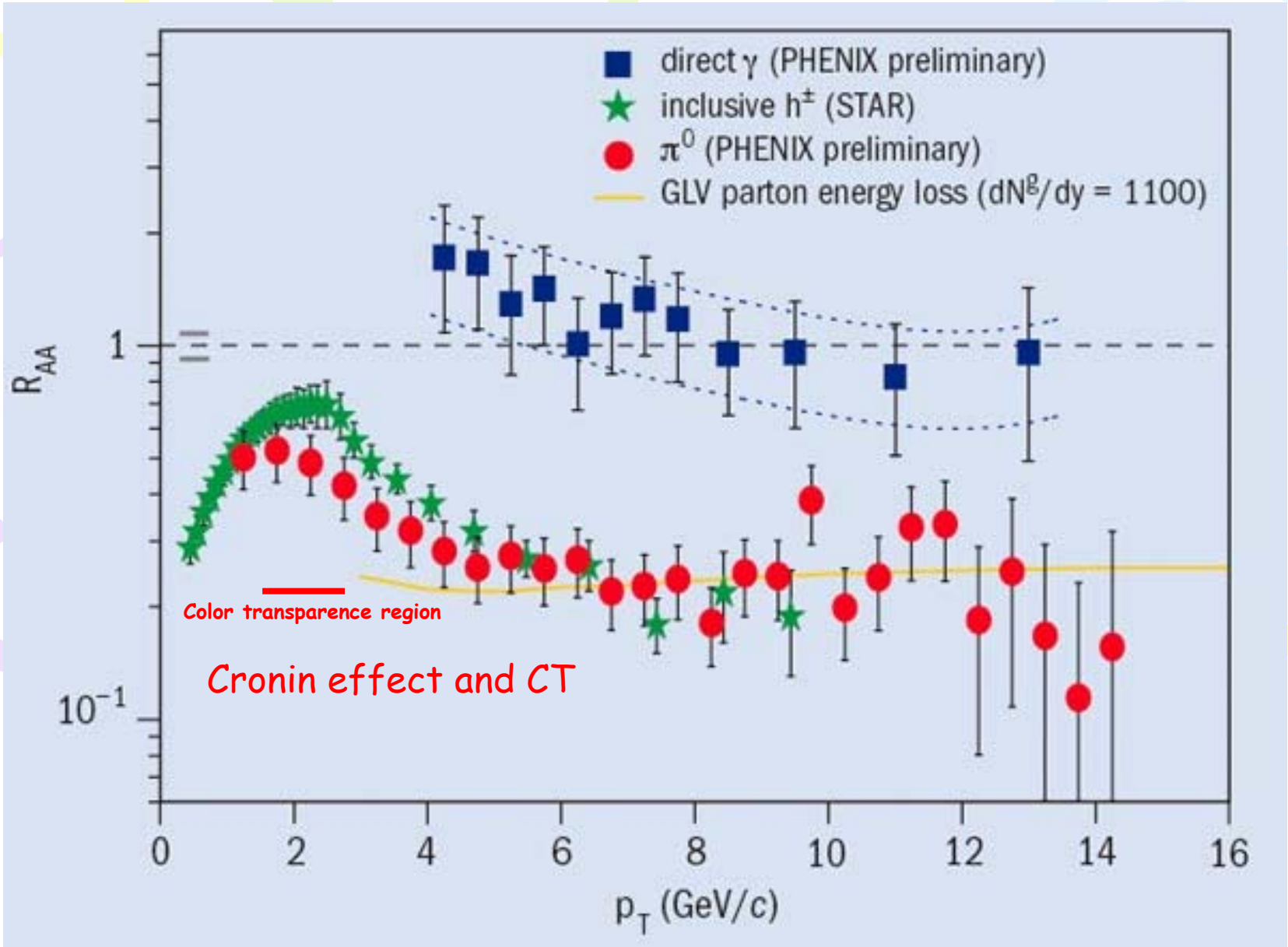

SLAC-PUB-13082
January 2008

Evidence for Color Transparency and Direct Hadron Production at RHIC *

Stanley J. Brodsky
Stanford Linear Accelerator Center, Stanford University, Stanford, California 94309

The QCD color transparency of higher-twist contributions to the inclusive hadroproduction cross section, where the trigger proton is produced directly in a short-distance subprocess, can explain several remarkable features of high-p_T proton production in heavy ion collisions which have recently been observed at RHIC: (a) the anomalous increase of the $p \to \pi$ ratio with centrality (b): the more rapid power-law fall-off at fixed $x_T = 2p_T/\sqrt{s}$ of the charged particle production cross section in high centrality nuclear collisions, and (c): the anomalous decrease of the number of same-side hadrons produced in association with a proton trigger as the centrality increases. These phenomena illustrate how heavy ion collisions can provide sensitive tools for interpreting and testing fundamental properties of QCD.

The main questions for DINR at PANDA

Do we see multiquark states inside nuclei or it's SRC of nucleons?

Which properties of these objects?

S.S. RNP 2005 Proceedings
nucl-ex/0604014

- average number of baryons accompanied high p_T cumulative particle production and its $s_{cumulat}$ dependance;

- average multiplicity accompanied high p_T cumulative particle production and its $s_{cumulat}$ dependance;

- $s_{cumulat}$ dependence of polarization characteristics (analyse power, asymmetry and so on), for SRC mechanism will be scaling repeating effects for free nucleon-nucleon interactions;

- coincidence cross sections of high p_T cumulative particle production with prediction of the "quark counting rules" [9] when using Stavinsky's variables.

High p_T road (E850/EVA)

p + "D"

$$\bar{p}_0 + \bar{k} = \bar{p}_1 + \bar{p}_2$$

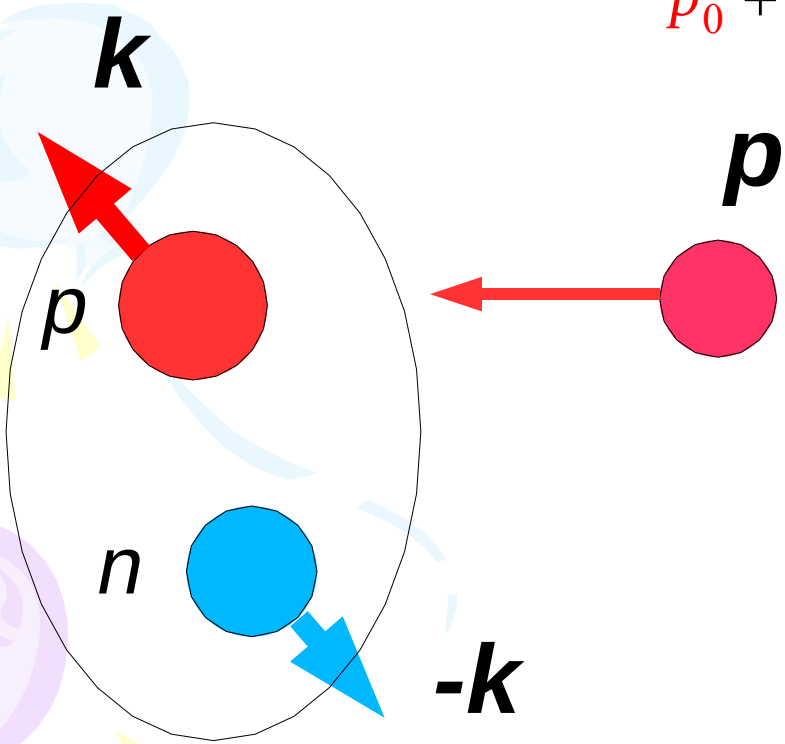

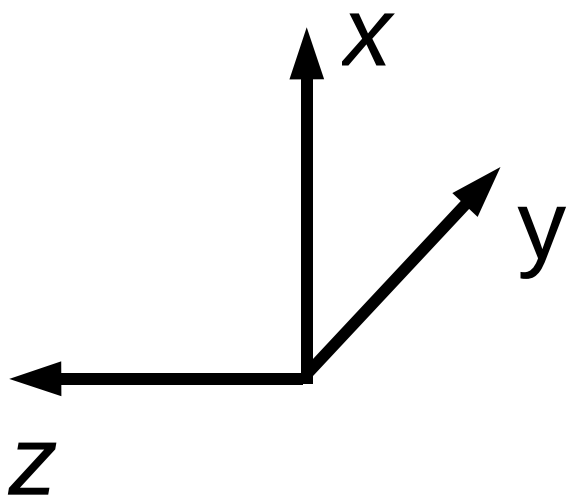

E850/EVA (BNL)

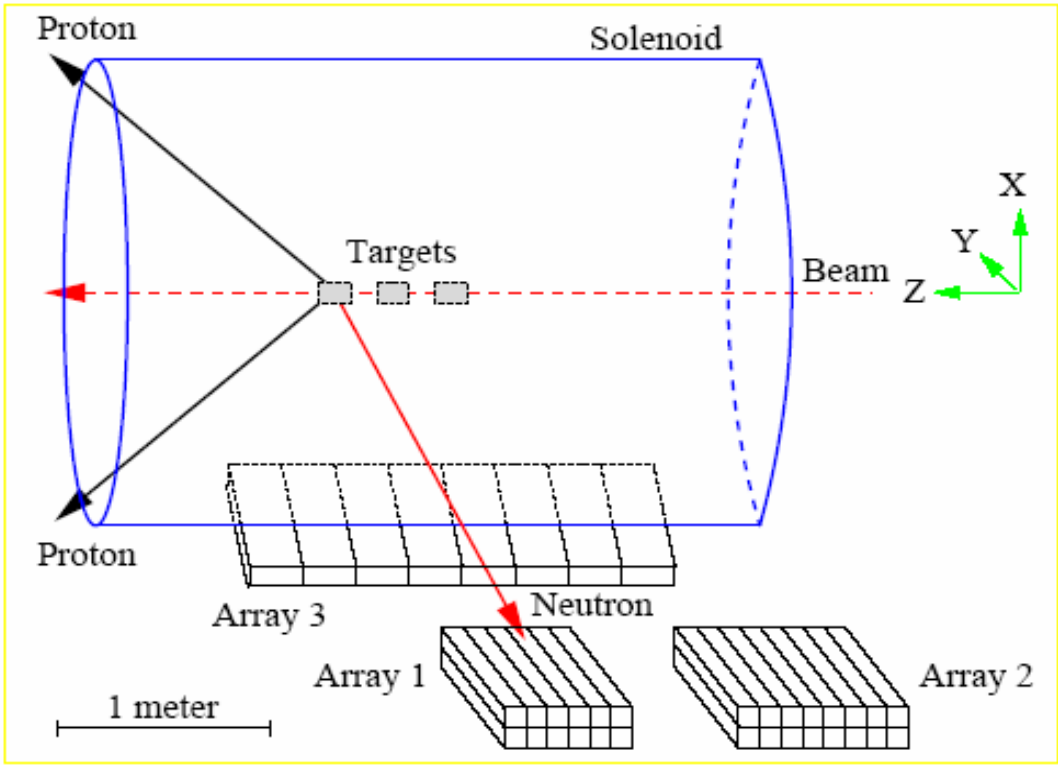

Figure I.3: A schematic view of the EVA solenoid and the neutron counters in the 1998 measurement.

n-p Short-Range Correlations from $(p, 2p + n)$ Measurements

A. Tang,[1] J.W. Watson,[1] J. Aclander,[2] J. Alster,[2] G. Asryan,[4,3] Y. Averichev,[8] D. Barton,[4] V. Baturin,[6,5] N. Bukhtoyarova,[4,5] A. Carroll,[4] S. Gushue,[4] S. Heppelmann,[6] A. Leksanov,[6] Y. Makdisi,[4] A. Malki,[2] E. Minina,[6] I. Navon,[2] H. Nicholson,[7] A. Ogawa,[6] Yu. Panebratsev,[8] E. Piasetzky,[2] A. Schetkovsky,[6,5] S. Shimanskiy,[8] and D. Zhalov[6]

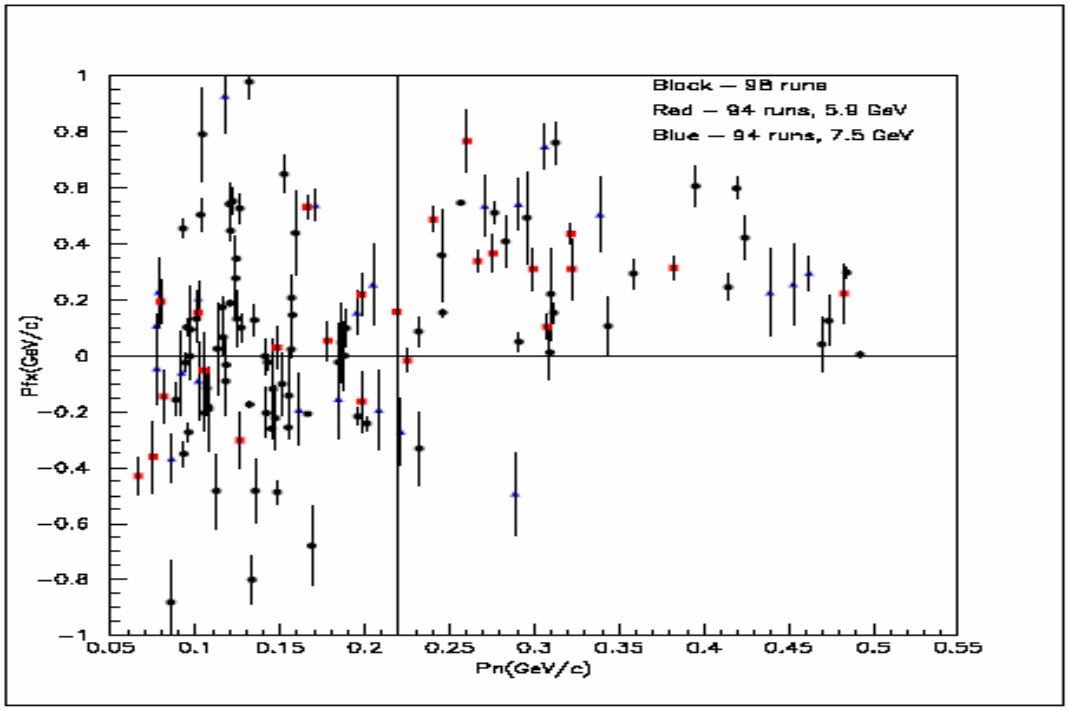

Figure I.5: The vertical component of the target nucleon momentum vs. the total neutron momentum.The positive vertical axis is the upward direction. The events shown are for triple coincidences of the neutron with the two high energy protons emerging from the QE C$(p, 2p)$ reaction. The squares are for the 5.9 GeV/c incident beam and the triangles are for 7.5 GeV/c. The dots are preliminary unpublished data from the 1998 runing period. We associate the events in the upper right corner with NN SRC.

Сечения квазибинарных процессов с большими p_T должны вести себя согласно правилам кваркового счета.
Как это будет связано с переменными Ставинского, когда исследовать кумулятивные процессы с большими p_T?

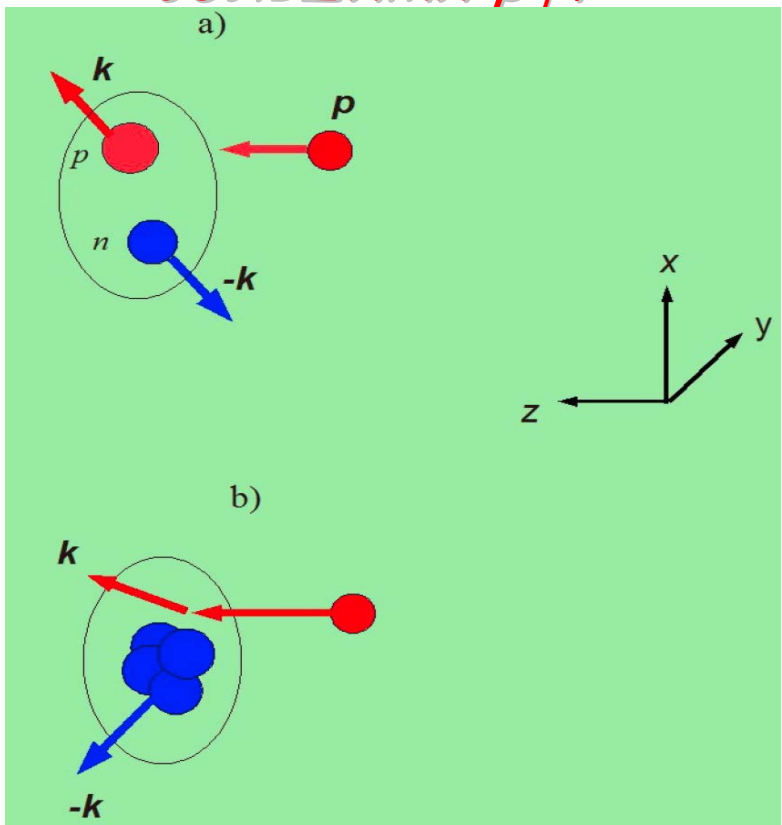

Простейшая постановка эксперимента

pA->p+?

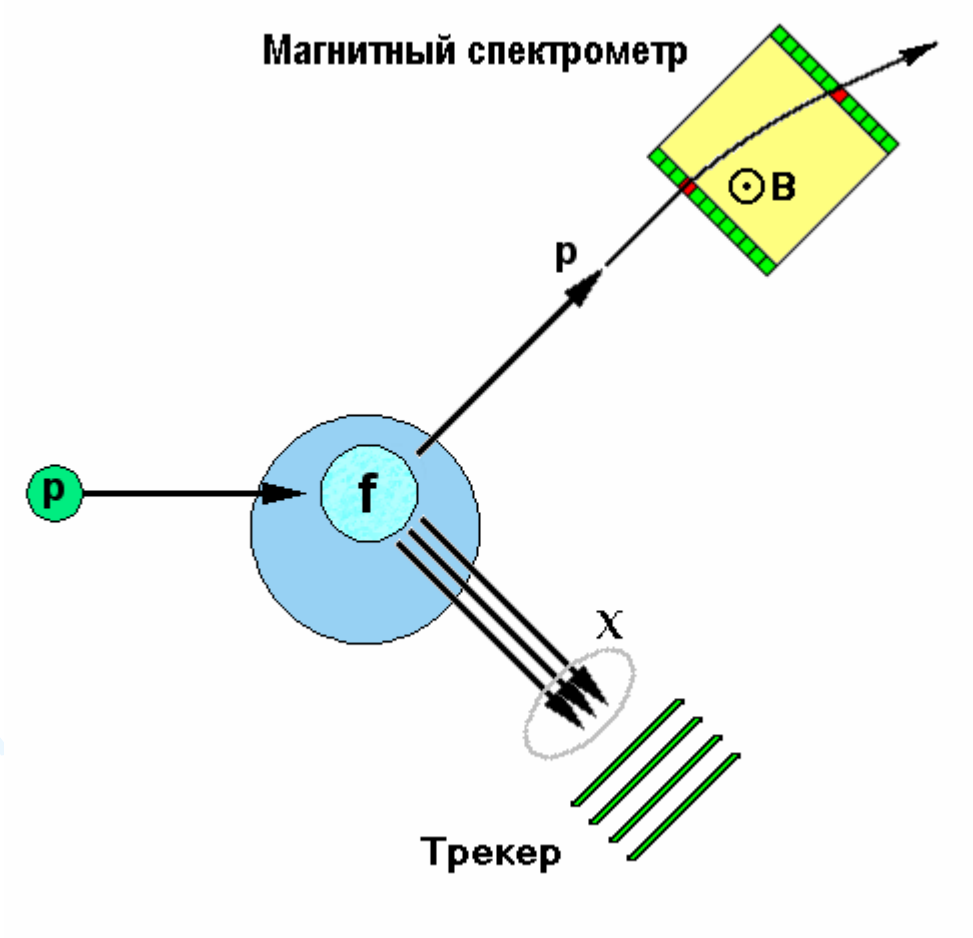

We can see the cold QG phase in ordinary nuclear mater and highlight this state in **pA-** and **AA-collisions**. This state directly connected with properties of the core for **NN-interaction**. We don't know well **NN-interaction** in overlapping range.

RHIC Physics: 3 Lectures*

+ CERN Yellow Report 2007-005, p.75

Larry McLerran

Physics Department PO Box 5000 Brookhaven National Laboratory Upton, NY 11973 USA

September 13, 2003

The Evolving QCD Phase Transition

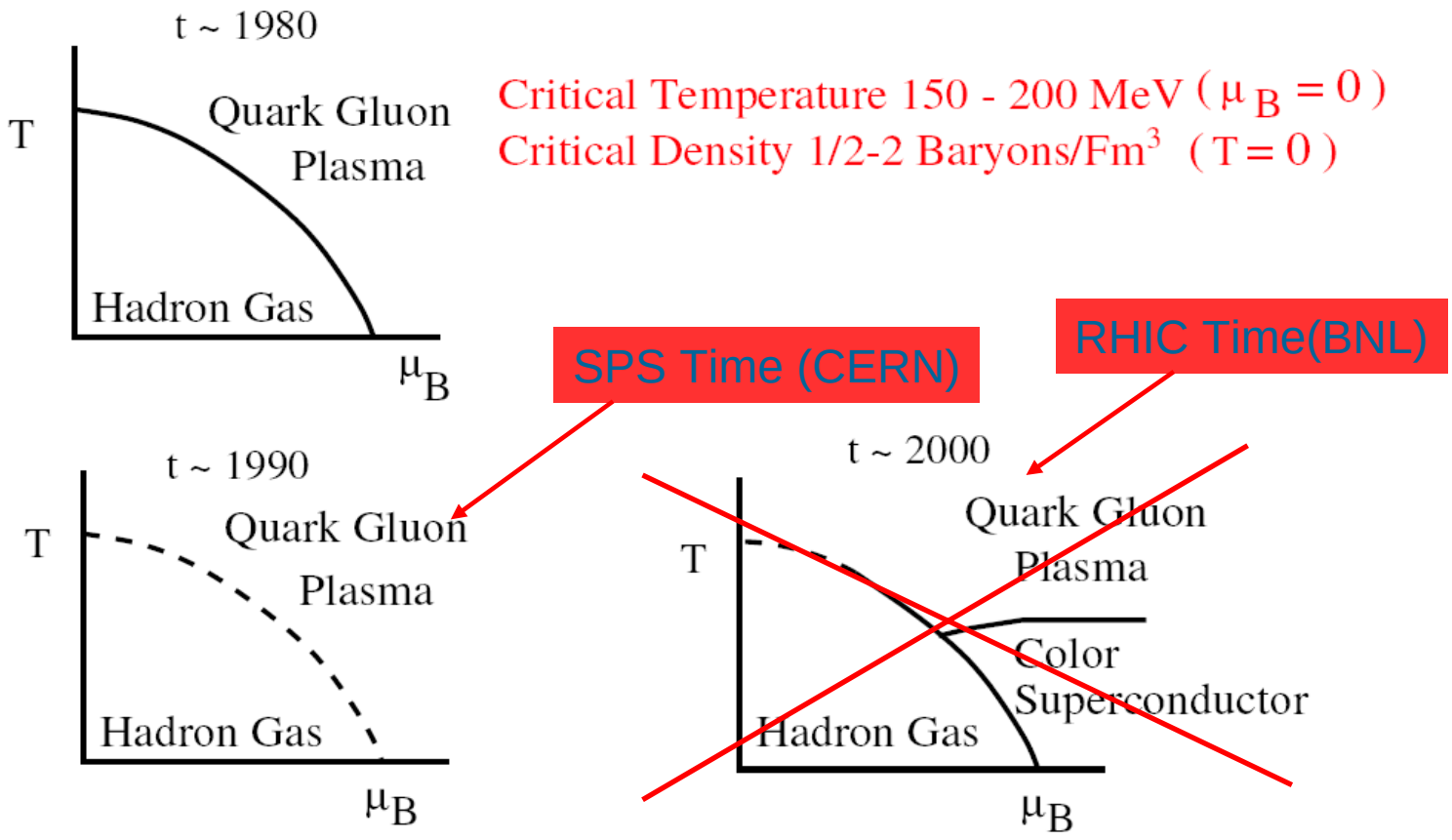

Figure 4: A phase diagram for QCD collisions.

QCD phase diagram

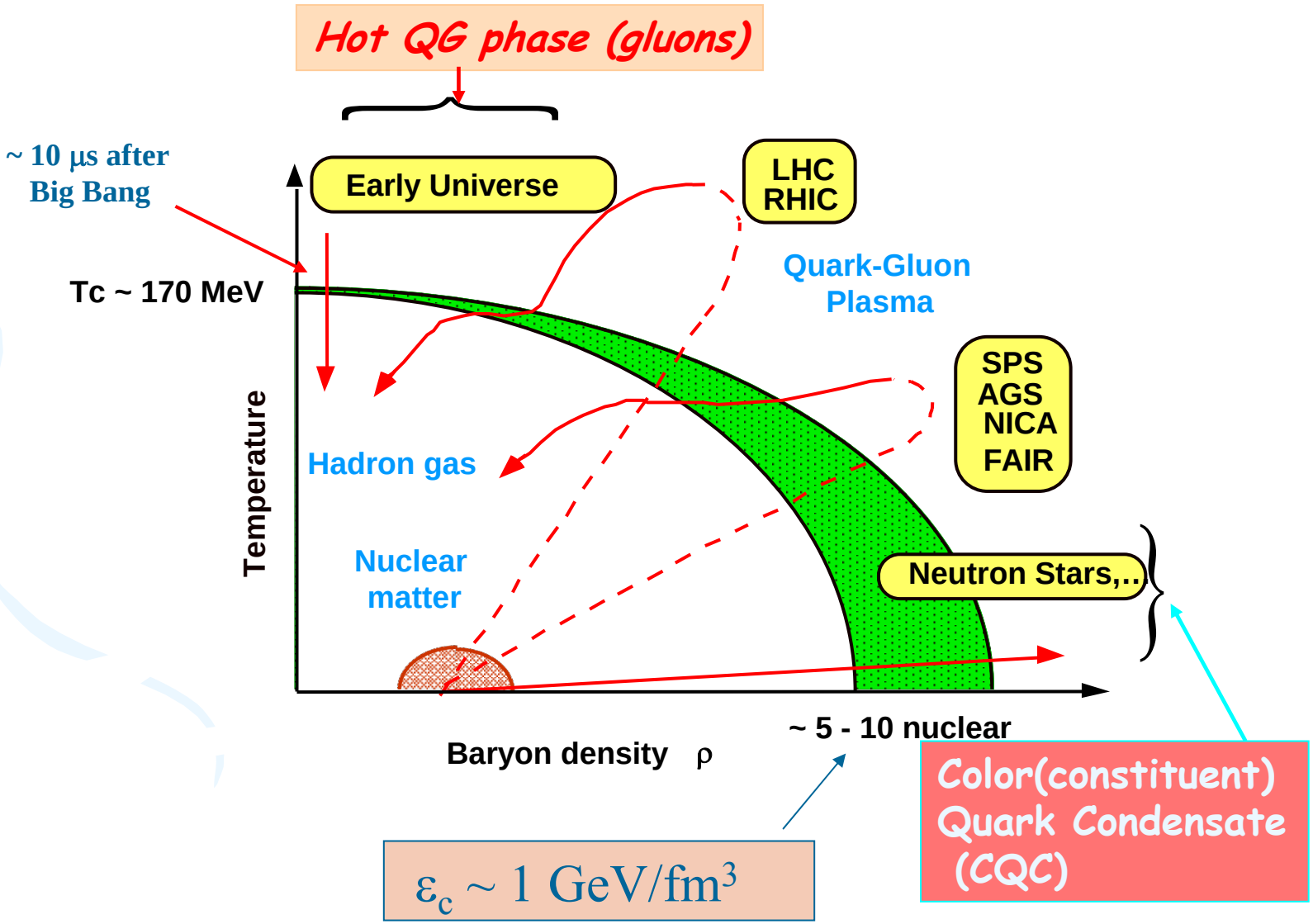

astro-ph/0604422 v1 20 Apr 2006

FRIDOLIN WEBER,* ALEXANDER HO,† RODRIGO P. NEGREIROS,‡
PHILIP ROSENFIELD§

$H \sim 10^{17}$ Gs

$E \sim 10^{19}$ V/cm

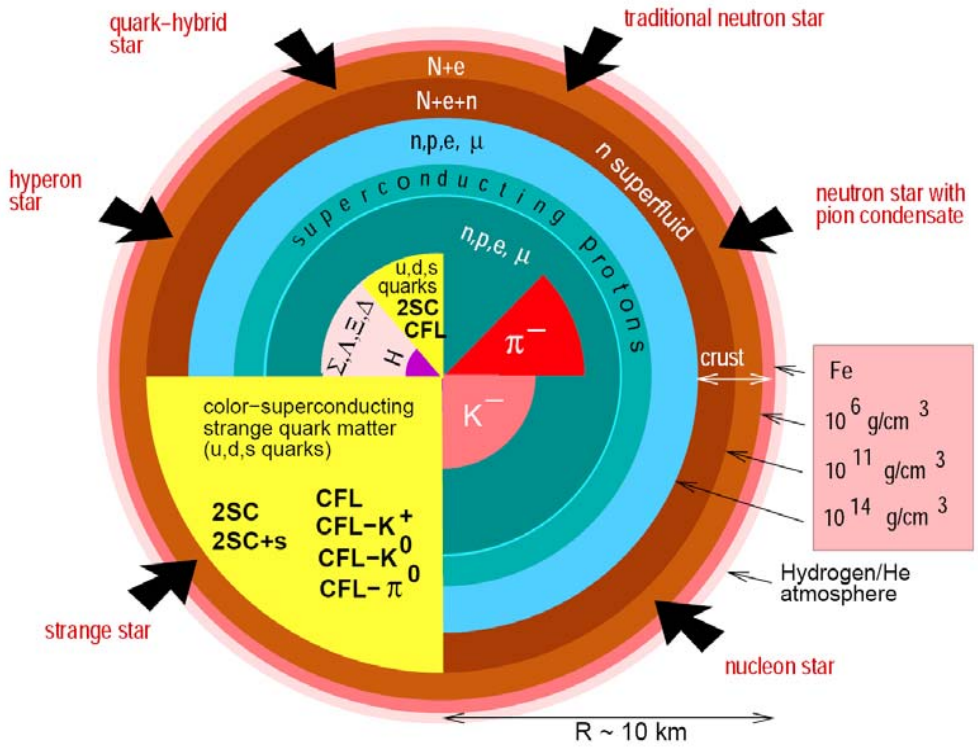

Fig. 1. Competing structures and novel phases of subatomic matter predicted by theory to make their appearances in the cores ($R \lesssim 8$ km) of neutron stars[4].

significant range of chemical potentials and strange quark masses[51]. If the strange quark mass is heavy enough to be ignored, then up and down quarks may pair in the two-flavor superconducting (2SC) phase. Other possible condensation patters

color–superconducting strange quark matter (u,d,s quarks)

K. Rajagopal and F. Wilczek, *The Condensed Matter Physics of QCD*, At the Frontier of Particle Physics / Handbook of QCD, ed. M. Shifman, (World Scientific) (2001).
M. Alford, Ann. Rev. Nucl. Part. Sci. **51** (2001) 131.

Нам необходимо ответить на два вопроса:

- есть ли многокварковые состояния в обычной ядерной материи или реализуется сценарий SRC(ферми-движение)?

- какие свойства многокварковых состояний или нуклонов в сильно неравновесном случае (SRC-сценарий)?

Исследование сечений в области предельно больших p_T(и $x \geq 1$) в инклюзивных, эксклюзивных и полуэксклюзивных реакциях могут однозначно ответить на вопрос о существовании многокварковых состояний в ядерной материи и, если они существуют, помочь исследовать свойства этих состояний.

Какая должна быть программа исследований?

Задачи для PANDA

Кумулятивные процессы в полуэксклюзивной и эксклюзивной постановке в области предельно больших p_T (природа CT и кумулятивных явлений, подпороговое рождение J/Ψ …)

Спасибо за интерес к этим проблемам!

"spin crisis" of 70's

A.D.Krish hep-ex/0511040

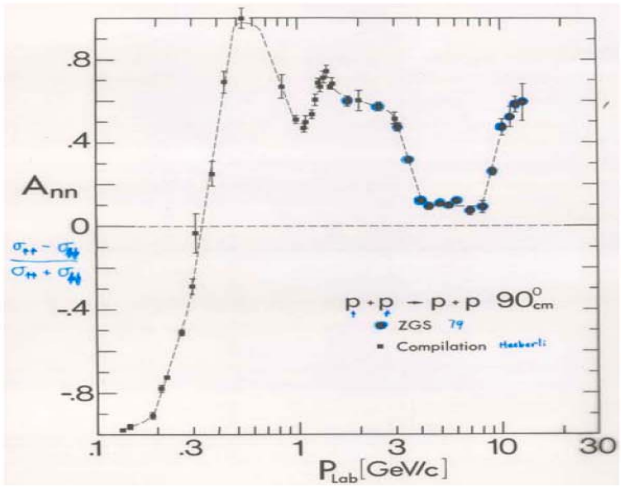

Figure 4: A_{nn} is plotted against P_{Lab}.

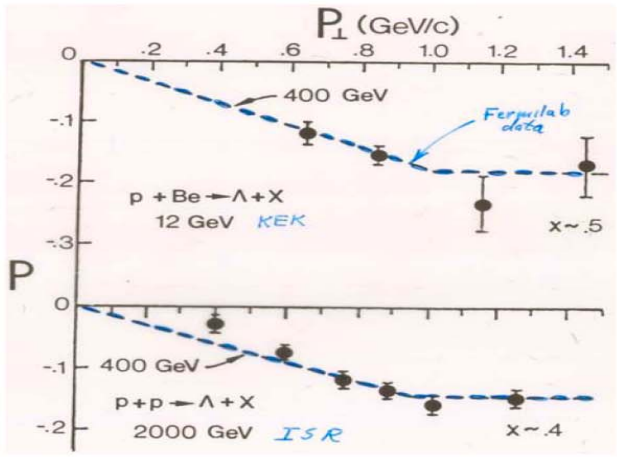

Figure 6: The Λ polarization is plotted against P_t^2.

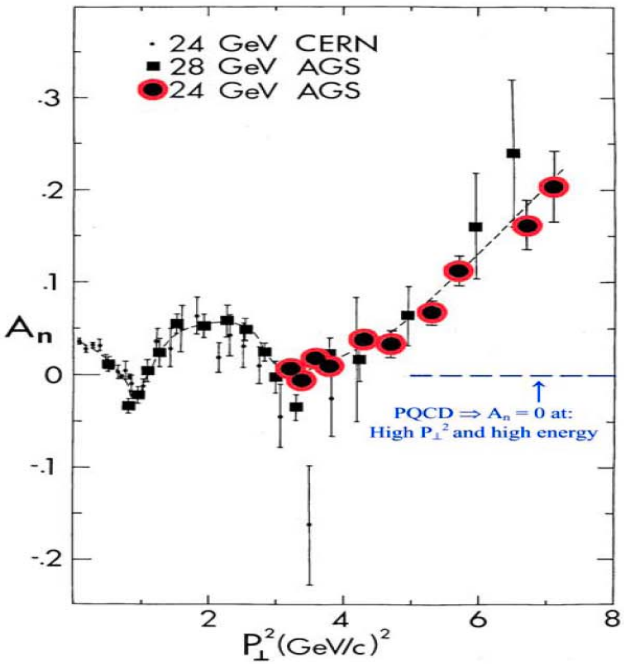

Figure 5: A_n is plotted against P_t^2.

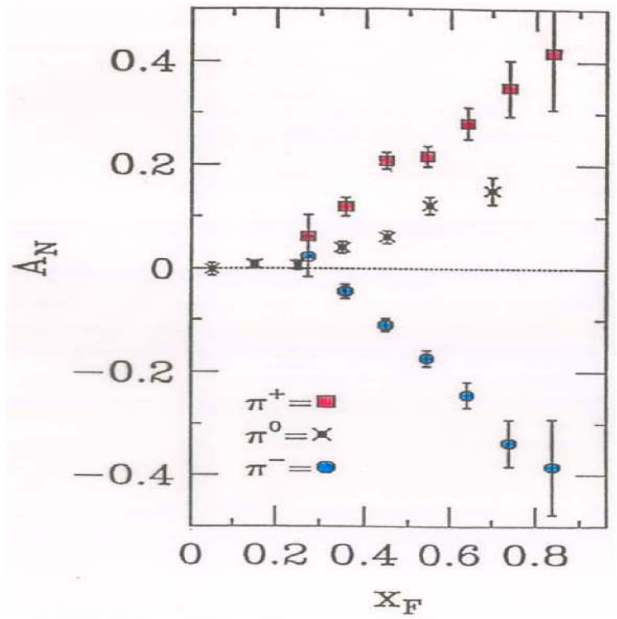

Figure 7: A_n is plotted against X_F for inclusive π-meson production.